Received: 25 April 2022 | Revised: 31 May 2022 | Accepted: 14 June 2022

DOI: 10.1002/tox.23610

RESEARCH ARTICLE

ENVIRONMENTAL TOXICOLOGY WILEY

Histopathological evaluation of the interrenal gland (adrenal homolog) of Japanese medaka (*Oryzias latipes*) exposed to graphene oxide

Asok K. Dasmahapatra[1,2] | Paul B. Tchounwou[1]

[1]RCMI Center for Environmental Health, Jackson State University, Jackson, Mississippi, USA

[2]Department of Biomolecular Sciences, Environmental Toxicology Division, University of Mississippi, Oxford, Mississippi, USA

Correspondence
Paul B. Tchounwou, RCMI Center for Environmental Health, Jackson State University, 1400 JR Lynch Street, Jackson, MS 39217, USA.
Email: paul.b.tchounwou@jsums.edu

Funding information
Jackson State University; CREST Center for Nanotoxicity Studies, Grant/Award Number: HRD 1547754; National Science Foundation; RCMI Center for Health Disparities Research, Grant/Award Number: 1U54MD015929; RCMI Center for Environmental Health, Grant/Award Number: G12MD07581; NIH/NIMHD

Abstract

Due to unique physicochemical properties and wide industrial and biomedical applications, graphene oxide (GO) is ubiquitous in the aquatic ecosystem. Using Japanese medaka (*Oryzias latipes*) fish as a model, we previously demonstrated minimal endocrine disrupting (ED) effects of GO on reproductive organs, and thyroids. Current study investigated the ED-effects of GO on the interrenal gland (IRG) of medaka. Breeding pairs of adult male and female fish were exposed to 0 mg/L (control) or 20 mg/L GO by continuous immersion for 96 h, or to 0 or 100 μg/g GO by intraperitoneal administration. Also, 1 day post-hatch (dph) larvae were exposed to different concentrations of GO (2.5–20 mg/L) for 96 h. IRG was evaluated by immunohistochemical techniques after 21 days depuration in adults and 6 weeks in larvae. IRG cells were counted and the nuclear area was measured in hematoxylin–eosin stained sections using ImageJ software. We found that IRG is distributed adjacent to the posterior cardinal vein and its branches within the head kidney. Columnar/oval shaped periodic acid-Schiff negative, tyrosine hydroxylase positive cells are arranged either in a single, or in groups, sometimes encircling a sinusoid, or in a straight chord, laying adjacent to the endothelium of the cardinal vein, and having eosinophilic cytoplasm with round/oval basophilic nuclei. GO effect on nuclei and cell population in IRG was inconsistent; depending on exposure route, sex, and/or age of the fish. Also, because of its high adsorptive property and sharp edges, GO probably agglomerated on IRG, and induced physical injury, and ED effects.

KEYWORDS
endocrine disrupting effects, graphene oxide, interrenal gland, Japanese medaka

1 | INTRODUCTION

The safety of chemical compounds that are disposed into the environment has been a concern for last few decades of the 20th century. Regulatory agencies like US Environmental Protection Agency (USEPA), Organization of Economic Cooperation and Development (OECD), and others, were unable to keep track with the rate of new compounds being released annually into the global environment.[1] Many of these compounds are known as endocrine disruptors (ED) that induced disorders in the structures and functions of the

endocrine organs either directly or indirectly. For the past several years, significant efforts have been made by OECD and USEPA to develop strategies for screening and identifying endocrine disrupting chemicals (EDCs) using model organisms living in different ecosystems.[2] Recently, over 600 compounds have been enlisted in a database as EDCs with reported evidence on humans and rodents.[3] However, a vast majority of chemicals have not yet been properly assessed for their potential impact on the endocrine systems.

In recent years, graphene oxide (GO), an oxidized derivative of graphene (an allotrope of carbon), due to its unique properties has been extensively used in industries, and human health.[4–10] An estimated 700 tons of graphene are produced per year in the United States and China alone[11] and due to low production cost these numbers are expected to increase as new technologies emerge. Inevitably, graphene nanomaterials are released into the environment during manufacturing, transportation, and public use.[12] When released into the water, graphene materials will interact with a variety of environmental (physicochemical as well as biological) factors and possibly causing significant adverse effects to the environment as well as to the ecosystem. Recently, the Water Quality Analysis Simulation Program 8 (WASP8) has reported a significant accumulation of GO in the water and sediments of four aquatic ecosystems (a seepage lake, a coastal plains river, a piedmont river, and an unstratified wetland lake) of the Southern United States. The study indicated that it will take 37+ years for lakes and 1–4 years for rivers to reduce graphene nanomaterial concentration by 50%.[9] These studies suggested that carbon-based nanomaterials have the potential for long-term effects on aquatic organisms. Many studies also indicated that graphene nanomaterials exhibit several unique modes of interaction with biomolecules such as nucleic acids, lipids and fatty acids, protein and peptides, as well as sugars[13] that cause a generation of reactive oxygen species (ROS) leading to oxidative stress in target cells.[14] Therefore, it is necessary to evaluate the toxic potential of GO in all possible ways using multiple physical, chemical, and biological techniques and models. Until now, the toxicological studies in GO are very limited, and these studies are yet to confirm GO as a potential EDC. Moreover, GO has been found to be a potential thyroid endocrine disruptor in tadpoles of *Xenopus laevis*,[15] even though contradicted by a recent study.[16]

Our laboratory has been evaluating GO, as a potential EDC using Japanese medaka fish (*Oryzias latipes*), as our experimental model.[17–23] We have demonstrated that the males of medaka fish are more sensitive to GO than the females. From our histopathological evaluation of the gonadal structures and thyroid follicles, we found that the damages observed after GO administration was mainly due to aggregation/agglomeration of GO on or within the organs rather than directly acting as an EDC.[18,19,22,23] Our other investigation of GO effect on the sex reversal (SR) of medaka larvae showed no apparent EDC effect.[20,21] In the present study, we have extended our investigations on the histopathology of the IRG of medaka adults and larvae exposed to different concentrations/doses of GO either by a single intraperitoneal (IP) injection or by 96 h continuous immersion (IMR). In fish, the IRG is considered as the adrenomedullary homolog of the mammalian adrenal gland. Our objective is to evaluate the potential EDC effects of GO on IRG, a significant member of the hypothalamus-pituitary-adrenal (HPA) axis in fish. We hypothesize that GO, due to its high adsorption property and sharp edges, if accumulated/agglomerated or in physical contact with the IRG can induce structural damage and/or modulate the cell population and hence affect the hormonal balance through HPA axis and steroidogenic pathways which may potentially disrupt endocrine-related cellular functions.

2 | MATERIALS AND METHODS

All the experimental animal protocols (# IBC 08-01-17 and IBC 09-01-17) were approved by the Institutional Animal Care and Use Committee (IACUC) of the Jackson State University, Jackson, MS.

2.1 | GO preparation

The GO compounds used in the experiment were either synthesized in the laboratory[18,19] or obtained from a commercial source (Sigma-Aldrich, St. Louis, MO). Before addition to the culture, GO (2 mg/ml or 2000 mg/L, dispersed in water; Sigma-Aldrich, St. Louis, MO) was diluted to desired concentration (20 mg/L which is equivalent to 20 μg/ml; 100-fold) by embryo rearing medium (ERM; 17 mM NaCl, 0.4 mM KCl, 0.6 mM $MgSO_4$, 0.36 mM $CaCl_2$, pH 7.4) for larvae or in balanced salt solution (BSS; 17 mM NaCl, 0.4 mM KCl, 0.3 mM $MgSO_4$, 0.3 mM $CaCl_2$, pH 7.4) for adults. For IP injection, a stock solution of 2 mg/ml GO, synthesized in the laboratory,[18] was made in nanopure water which is consistent with the concentration of GO obtained from the commercial source (2 mg/ml). The solution of GO (both 20 and 2000 mg/L) was sonicated for 5 min (2 s on -1 s off pulse, 225 w) using a probe sonicator (ultrasonicator LPX 750, Cole Palmer, Chicago, IL) in ice temperature and further diluted to desired concentration when necessary (for larvae). The sonicated nanomaterial was further checked by transmission electronmicroscope at the Electron Microscopy Core laboratory at the Jackson State University, Jackson, MS.[18–21]

2.2 | Animal maintenance and GO exposure

The maintenance of the adult Japanese medaka fish colony (Orange red variety, Hd-rR strain) at the Jackson State University, Jackson, MS, was described previously.[18,19] Briefly, the adult fish used as breeders were maintained in 35 L tanks in 25 L BSS at 25 ± 1 ° C with 16 h L: 8 h D light cycle. The media was recirculated through pumps and filtered through disposable bio and carbon filters. BSS was refreshed every 2–3 weeks as and when necessary, depending on the pH (6.5–8.5) and ammonia concentration (1–3 ppm). The fish breed successfully in this environment and the eggs were generally collected within 1–3 h after the light turned on. The embryos were reared in ERM and generally hatched within 10–12 days after post fertilization

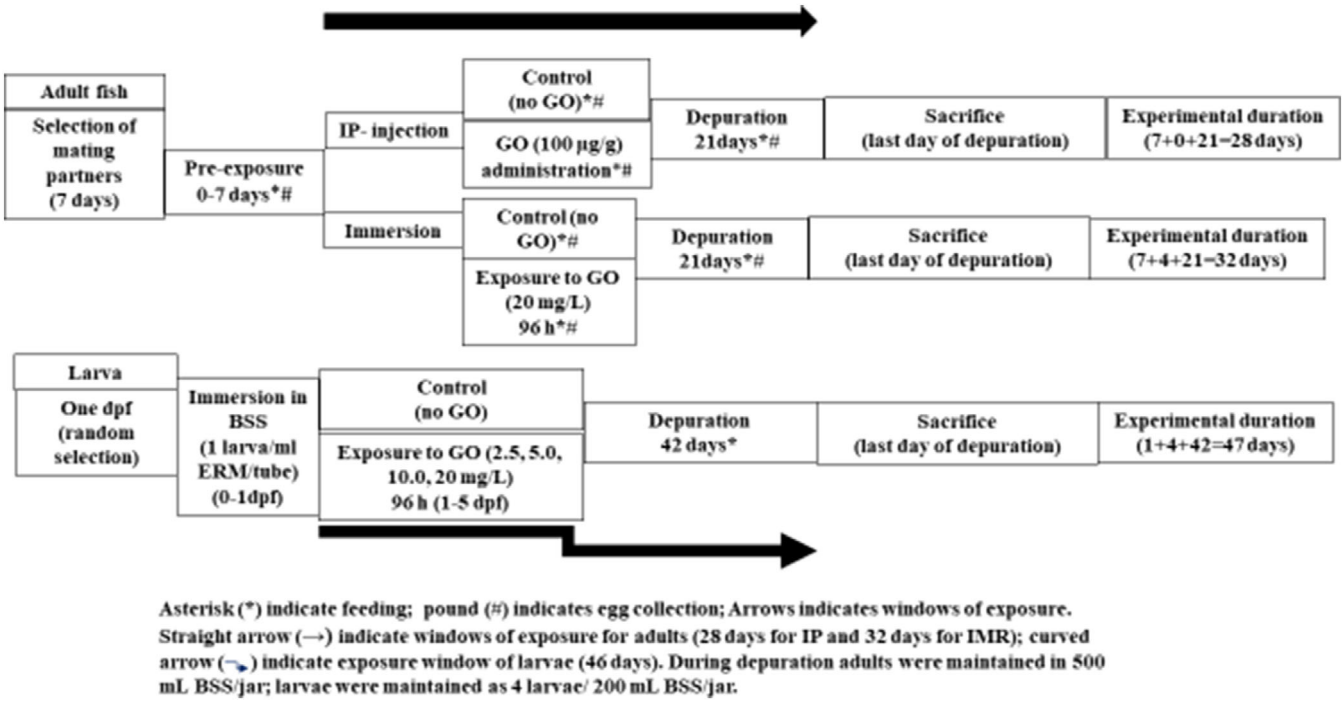

FIGURE 1 Schematic diagram of the graphene oxide (GO) exposure paradigm to adults and larvae of Japanese medaka fish. Sexually mature, reproductively active, adult male, and female medaka fish as a breeding pair (one male and one female) were maintained in 500 ml balanced salt solution (BSS) in a 1 L glass jar in standard laboratory conditions (light cycle 16 h light 8 h dark; 25 ± 1°C. Eggs were collected (both fertilized and unfertilized) for 7 consecutive days before the exposure to GO either by IP-injection (100 µg/g; single injection) or by immersion (20 mg/g; 96 h continuous with refreshing of media every 24 h). Food was given to adult fish during the exposure period. Control fish were injected with vehicle (water) or immersed in 500 ml of BSS. The media was refreshed every day. After GO exposure (either by injection or immersion) the fish were transferred to 500 ml of fresh BSS (no GO) and allowed breeding (same pair), and maintained 21 days in a GO-free environment with regular feeding and refreshing of the media. The collections of eggs from individual breeding pairs continued. On 21st day post-treatment (3 weeks depuration) the fish were sacrificed and the trunk was preserved in 4% paraformaldehyde in 20 mM phosphate buffered saline for histological examination of the interrenal gland (adrenal homolog in mammals) as well as gonads (testis and ovary). one (1) day post-hatch (dph) medaka fries were exposed to different concentrations of GO (0, 2.5, 5.0, 10.0, and 20.0 mg/L) continuously for 96 h in 1 ml ERM without any external food. The media refreshed every 24 h. After treatment the larvae were transferred to 500 ml glass jars in 200 ml BSS(4 larvae) and maintained in the laboratory with feeding for 6 weeks (42 days) and frequent change of media, depending on the pH and ammonia content. On 47th dph, the larvae were sacrificed and trunk regions were preserved in 4% PFA in 20 mM PBS and used for IRG and gonads. The tail used for genotyping.

(dph). The development and staging of the experimental fish were characterized as previously described by Iwamatsu.[24]

2.3 | Exposure of adult fish to GO

Previously, we have injected GO (25–200 µg/g; single intraperitoneal injection) to the sexually mature and reproductively active adult medaka male and female fish and evaluated the reproductive and developmental effects after 3 weeks (21 days) post-injection.[18,19] In the present study, we have considered only one injected group (100 µg/g; 7 pairs injected fish) along with the controls for evaluation of IRG (please see the schematic diagram in Figure 1). Since injection is not a good method for EDC studies in aquatic animal models, in the current study, we have exposed the reproductively active adult fish in GO solution (20 mg/L in BSS; the highest concentration of GO we used in larval exposure; the concentration of GO for in vitro exposure was initially based on Mullick-Choudhury et al.,[25] by IMR). Before exposure, both partners (one male and one female) were maintained for 1 week in 500 ml BSS in the laboratory condition in 1 L glass jars. The media was changed every day. After 1 week of acclimatization, when both male and female fish breed successfully (evaluated by counting the eggs as fertilized and unfertilized eggs), each breeding pair was immersed in 500 ml of BSS in 1 L glass jars for 96 h containing either GO (20 mg/L; sonicated as described above) or no GO (control). The fish were fed during the exposure period. The GO, even after sonication, when added to the BSS, precipitated at the bottom of the jars after 3–4 h of treatment. Therefore, the media was refreshed every day. After 96 h of exposure the fish were transferred to 500 ml of fresh BSS (no GO) and allowed breeding (same pair), and maintained 21 days in a GO-free environment with regular feeding and refreshing of the media. On 21st day the fish were sacrificed and the trunk was preserved in 4% paraformaldehyde (PFA) in 20 mM PBS for histological examination of the IRG (adrenal homolog in mammals) as well as gonads (testis and ovary). The fish bred successfully in all conditions of GO exposure (pre-exposure, exposure, and post-

exposure) and produced viable eggs. No death of the breeding pair was observed during the exposure/post-exposure period. The histopathology of IR axis of the fish exposed to GO by IMR was also compared with the fish administered GO (100 μg/g) by IP-injection.[18,19] The gonad histology was used to confirm the phenotypic sex of the breeding pairs.

2.4 | Exposure of Larvae

Previously we exposed 1 dph medaka fries (Iwamatsu Stage 40, 1st fry stage) to different concentrations (2.5, 5, 10, 20 mg/L in ERM) of GO (Sigma-Aldrich, St. Louis, MO) for 96 h continuously by IMR and assessed the EDC activities of GO on gonads (testis and ovary) and thyroids after 6 weeks post-treatment.[20–23] In this study, we have evaluated the IRG of some of these larvae by histological/histochemical methods. Due to technical problems, we were unable to track the IRG of all the larvae we used during our previous experiments. Briefly, the experimental fries (1 dph larvae) were kept fasting (no exogenous food) during the exposure period (control; no GO, treatments 2.5–20 mg/ml GO; 96 h continuous; 1–5 dph). On 5 dph, survived fries were transferred to BSS and maintained in 500 ml glass jars (4 fries/200 ml BSS) in the laboratory (25 ± 1°C; 16 h light and 8 h dark light cycle). The larvae were fed during the depuration period. The mortality of the cultured fries/larvae was checked every day and the media changed once a week. The larvae (stages 42–43) were sacrificed after 42 days (47 dph) post-treatment (Please see the schematic diagram in Figure 1). The preserved trunk tissues in 4% PFA in 20 mM PBS that contain kidney were used for histological evaluation of the IR axis of medaka; the DNA extracted from post anal tail were used for genotype (XY/XX).[20,21] The phenotypic sex (testis and ovary) of the larvae was determined by gonad histology.[20,21]

2.5 | Phenotype and genotype determination of the adult and larvae

The phenotypic sex of an adult fish was based externally on the fin features (papillae of anal fin, furrow in dorsal fin and the shape of the fish) and internally by the histological evaluation of testis (male) or ovary (female). The phenotype and genotype of the larvae was determined by the methods described previously.[20,21] Due to sex-reversal observed in some of the phenotypes (male phenotype with XX genotype), the larvae were then categorized in to three groups; male (testis) phenotypes with XY genotype, male (testis) phenotypes with XX genotype (sex reversed), and female (ovary) phenotypes with XX genotype. We did not observe any female (ovary) phenotype with XY genotype. During data analysis, due to limited number of sex-reversed larvae, the XX genotypes having phenotypic testis (sex-reversed) were included as male larvae (testis) in phenotypic analysis and as XX larvae in genotypic analysis. The adults were categorized either as males or females based on their phenotypic features (externally by fin features and internally by gonad histology).

2.6 | Histology and histochemistry of interrenal gland

The trunk region of the medaka fixed in 4% PFA containing 20 mM PBS for 48 h (changed once after 24 h), was washed thoroughly in water. The washed tissues were dehydrated in graded alcohols, cleared in xylene and embedded in paraffin (58–60°C) and the serial sections at 5 μm thickness were cut in a manual rotary microtome (Olympus cut 4055). For light microscopic studies, cell sorting and nuclear area, the sections were used for hematoxylin and eosin (HE) staining; periodic acid-Schiff (PAS; Sigma-Aldrich, St. Louis, MO) technique was used for histochemical properties. For tyrosine hydroxylase (TH), the rate limiting enzyme of catecholamine synthesis that expressed in the adrenal medulla,[26] we have used immunohistochemical techniques using rabbit polyclonal anti-TH antibody (Sigma-Aldrich, St. Louis, MO) as primary antibody (please see below). The photomicrographs of the stained sections were taken in an Olympus CKX53 inverted microscope attached with a DP22 camera with CellSens software (Huntoptics &Imaging, Pittsburg, PA). The images captured in different regions of the IRG by HE staining were used for counting the cells and a particular area of the IRG was determined by ImageJ software (http://www.imagej.nih.gov/ij) For quantitative analysis of the structural impairments made on the IRG of medaka, the data were expressed as number of cells/mm^2 area of the IRG. Although the IRG of medaka consists of both interrenal cells and chromaffin cells,[27] based on the straining intensity of the nuclei, in the present study, we have further categorized the counted HE stained IRG cells as the cells with deep-stained nuclei (DSN) and the cells with pale-stained (PSN) nuclei (please see the supportive information Figures 1A and S1a,b) instead of interrenal cells and chromaffin cells as described by Oguri.[27] The data were expressed as number of cells (either DSN or PSN)/mm^2 area of the IRG. The area that contain DSN and/or PSN cells in a particular region of IRG were determined by ImageJ software during total cell (DSN + PSN) count. Moreover, the nuclear area of DSN or PSN cells was also determined by ImageJ software.

2.7 | Tyrosine hydroxylase immunohistochemistry

For specific location of the IRG in the head kidney of medaka, we have used immunohistochemical technique for the detection of TH, the rate-limiting enzyme in catecholamine biosynthesis that expressed in the chromaffin cells of IRG using the method described by Shin et al.,[28] with some modifications. Briefly, tissue sections (5 μm thickness) on glass slides containing kidney with IRG were deparaffinized and brought to tap water. A 40 min antigen masking (antigen retrieval) was done in citrate buffer (pH 6.0) at 85–90°C. After washing in 0.1 M phosphate buffered saline- tween 20 (PBST), for blocking the endogenous peroxidases and alkaline phosphatases, the sections were treated with bloxall (Vector laboratories, Burlingame, CA) for 10 min at room temperature. After a brief wash with PBST, before the application of primary antibody, the sections were incubated with 3%

normal goat serum (Vector laboratories, Burlingame, CA) in PBST for 1 h at room temperature. Then the sections were incubated with primary antibody (polyclonal rabbit-derived anti-TH with a final dilution of 1:200 in 3% goat serum in PBST; Sigma-Aldrich, St. Louis, MO) overnight at 4°C. Parallel control sections on glass slides were incubated in identical condition in 3% goat serum-PBST without primary antibody. Sections were washed several times in PBST and incubated for 1 h at room temperature with biotinylated goat antirabbit secondary antibody (Vector laboratories, Burlingame, CA) diluted (1:200 for adults and 1: 300 for larvae) in PBS with 3% goat serum. Sections were washed again in PBS and incubated for 1 h at room temperature with avidin-biotin complex in PBS as recommended by the manufacturer (Vector laboratory, Burlingame, CA). The sections were washed several times in PBS and incubated for 1 h at room temperature with vectastain elite ABC reagent (Vector laboratory, Burlingame, CA). Sections were washed several times in PBS and incubated in room temperature for 5–10 min with freshly prepared peroxidase substrate (vector DAB) as recommended by the manufacturer (Vector laboratories, Burlingame, CA). After incubation the sections were washed in tap water and counter stained with hematoxylin, dehydrated in alcohol, cleared in xylene and mounted in permount (Fisher scientific; St. Louis, MO). The sections were evaluated and photographed under microscope. Antibody positive cells were deep-brown in color, even though some background color could still exist in renal tubules, especially in larvae.

2.8 | Statistical analysis

Data were analyzed using GraphPad prism version 7.04 (GraphPad Prism, San Diego, CA). We used descriptive analysis to evaluate nuclear area (μm^2) of IRG cells, and the distribution (number/mm^2) of these two cell types either alone (DSN and PSN) or total cells (DSN + PSN) at the IRG of Japanese medaka adults and larvae (47 dph) after HE staining. We used D'Agostino-Pearson (DP) or Shapiro-Wilks (SK) test to determine the normality of the data. If the data were normally distributed and meet the percepts of using a parametric test, we used one-way ANOVA followed by unpaired parametric "*t*" test including Welch's correction as a post hoc test. The statistical significance was defined as $p < .05$. If the normality test indicated that the data did not meet the criteria of using a parametric test, we performed the Kruskal-Wallis test followed by Mann-Whitney's test (nonparametric test) as a post hoc test and the level of significance adopted as $p < .05$. All the numerical data were expressed as mean ± *SEM*.

3 | RESULTS

3.1 | Evaluation of the IRG of medaka adults after GO exposure

The IRG in Japanese medaka is located in the head/cephalic kidney which is visible anterior to the swim bladder and in the anterio-dorsal part of the abdominal cavity. In adult medaka, the kidney can easily be divided into cranial (cephalic) and caudal (tail) region with a short trunk between the two. The organ (kidney) is covered by a capsule of dense fibrous connective tissue. The parenchyma is composed of renal units (glomerulus and tubules), IRG consisting interrenal (steroidogenic) and chromaffin (catecholamine synthesizing) cells, and lymphoid and hematopoietic units consisting melanomacrophase centers (MMC) and melanomacrophages and lymphocytes. The IRG is closely associated with the posterior cardinal vein and its branches within the kidney.[27] The trunk or tail kidney does not have any steroidogenic or chromaffin tissues, however, the renal units and the lymphoid tissues, MMC, and Stannius corpuscles (SC) are present either in the whole region or only in tail (SC) kidney.

Our light microscopic observation of HE stained sections of Japanese medaka adults indicated that the cells of IRG were arranged either in a single, or in groups (clumps), or in a straight cord, adjacent to the endothelium of the cardinal vein within in the cephalic kidney (Figures 2A–D and 3A–D; also please see the supporting information Figures S1a,b). Since the structural appearance of the IRG was a result of the plane of the section, in some occasions, this arrangement seems to be missing. The cords are more or less straight, 2–3 cells thick,[27] bordered by the lining endothelium of the adjacent sinusoids which sometimes contain variety of blood/immune cells. The shapes of the IR axis cells, depending on the plane of sections, appeared as columnar or oval, and were in contact with the hematopoietic tissue or separated from it by the sinusoids, where no connective tissue capsule could be observed. These cells have eosinophilic cytoplasm with round or oval basophilic nuclei and distinct nucleoli. Histochemically, the IRG cells were found to be negative for PAS (Figure 3), though the cilia of the proximal tubular cells in the kidney and the melanomacrophages in the immune units are PAS positive (Figure 4). The immunohistochemical observation indicated that TH (the rate-limiting enzyme of catecholamine synthesis) immunoreative cells are present in IRG of medaka (Figure 5; also please see Figures S4–S7). Depending on the HE staining intensity of the nucleus, we have further classified the IR axis cells into DSN and PSN cells (please see Figure S1a,b).

The histological (Figures 2 and 3), histochemical (Figure 4) and immunohistochemical (Figure 5) evaluations of the IRG of adult fish exposed to GO either by IMR (20 mg/L; 96 h continuous; Figure 2E–H) or by IP (100 μg/g; Figure 3E–H) were done after 3 weeks of depuration in a GO-free environment. We have observed that the differences in morphological features of the IRG of both male (Figure 2E,F) and female fish (Figure 2G,H) immersed in GO (20 mg/L) solution were found to be very minimum, most likely identical with the control (no GO) male (Figure 2A,B) and female fish (Figure 2C,D). However, the IP fish exposed to GO (100 μg/g) showed inconsistent structural derangement in several regions of the IRG (Figures 3E–H; S2a,b). The cord of the IRG in the affected regions became swelled and the shape of the cord appeared to become dumbbell with cellular deformities compared to controls (Figures S2a,b). Histochemical evaluation by PAS did not show any apparent change, however, in a few cases the fish exposed to GO, the cytoplasm of the IRG cells became pink (Figure 4C). Moreover, in a few occasions, the PAS positive

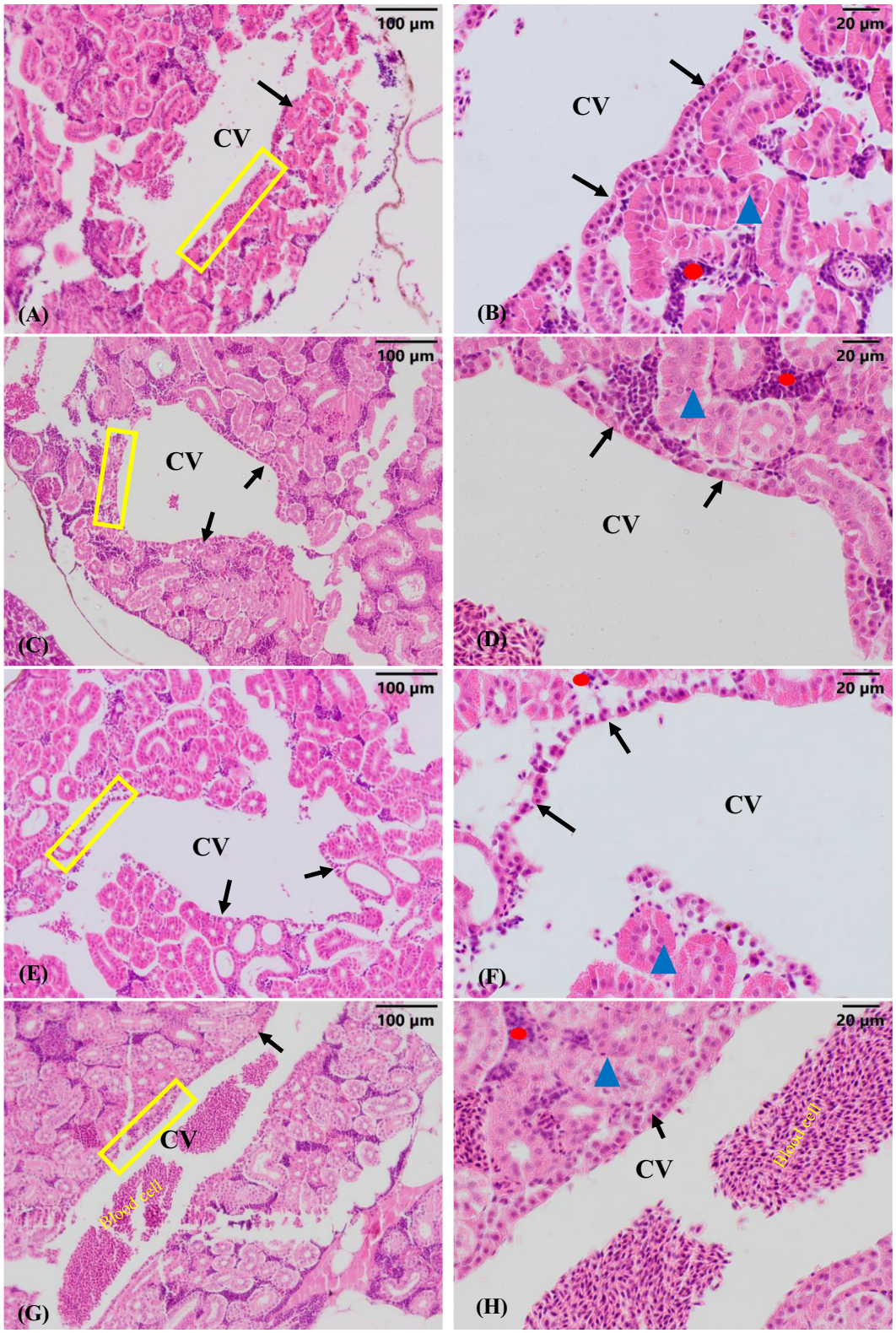

FIGURE 2 Histology of the interrenal gland (IRG) (adrenal homolog) of the adult Japanese medaka exposed to graphene oxide (GO) by immersion (IMR). Sexually mature and reproductively active adult male) and female medaka as breeding pairs were exposed to GO (20 mg/L in balanced salt solution [BSS]) by IMR continuously for 96 h and then maintained only in BSS (no GO) for 21 days in a GO-free environment. Control fish (Figures 2A–D) were maintained in identical condition with no GO. IRG (black arrows) was observed adjacent to the posterior cardinal vein passing through the head kidney. Representative figures are presented as: Figure 2A, IRG of control male fish; 2B, magnified region of the IRG of male fish square marked in Figure 2A; Figure 2C, IRG of control female fish; Figure 2D, magnified region of the IRG of female fish square marked in Figure 2C; Figure 2E, IRG of male fish exposed to GO; Figure 2F, magnified region of the IRG of male fish square marked in Figure 2E; Figure 2G, IRG of female fish exposed to GO; Figure 2H, magnified region of the IRG of female fish square marked in Figure 2G; CV, cardinal vein; black arrow, IRG; blue triangle: renal tubule (renal unit of the kidney); red circle: interstitial cells (lymphoid and hematopoietic units of the kidney).

melanomacrophage/MMC components (due to lipofuscin) are also seen in the IRG exposed to GO either by IMR (Figure 4D) or by IP (Figure 4G) (also please see, Figures S3a,b). Immunohistochemical studies indicated that despite structural impairments of the IRG by GO exposure, TH immunoreactive cells are present in the IRG of medaka and seems to have identical TH immunoreactivity as observed in control fish (Figures 5A–H; also see the Figures S4–S7).

3.2 | Distribution of IRG cells of Japanese medaka adults exposed to GO either by IMR or by IP-injection

For quantitative assessment of the structural impairments induced by GO, we have counted cells in different regions of the IRG of Japanese medaka irrespective of the nuclear staining intensity (DSN + PSN) and expressed as number of cells/mm^2 area of IRG (Figure 6). The average number of cells we were able to count in control (no GO) male fish immersed in BSS (no injection) is 30 033 ± 2558/mm^2 (n = 10 regions of IRG used for cell count) and for control female fish is 22 688 ± 1029/mm^2 (n = 25). For IP control (vehicle injected) male fish the number of IRG cells is 26 784 ± 904/mm^2 (n = 16) and for IP control female fish the numbers is 24 622 ± 904/mm^2 (n = 12) (Figure 6A). Further, we have divided these IRG cells as DSN and PSN and observed that the ratio of DSN/PSN cells in an IRG was inconsistently variable, even though the number of PSN cells in most of the cases remained higher than DSN cells (Figure 6B,C). Furthermore, for consideration of cellular functions, we have also evaluated the nuclear area of DSN and PSN cells in these experimental fish. Considering the route of exposure (IMR vs. IP- injection), and the sex of the experimental animals (male vs. female), in the adult fish, we have focused on the cell number (/mm^2) and the nuclear area (μm^2) of the experimental fish as the indicators of the structural impairments induced by GO in the IRG of Japanese medaka (Figure 6A–E).

Our data indicated that the experimental male and female fish exposed to GO (20 mg/L) by IMR were unable to document any significant differences (not significant; NS) in the number of IRG cells with the corresponding control males or females (control male vs. GO males; IMR; p = NS; control female vs. GO female; IMR; p = NS); however, in both male and female fish, when GO was injected IP (100 μg/g), the cell number (/mm^2) showed significant reduction in IRG cells, when compared with the corresponding controls (control male vs. GO male, IP, p < .05; control female vs. GO female, IP; p < .05) (Figure 6A). Moreover, our data indicated a gender-specific difference in IRG cell number between male and female fish (males have significantly higher number of cells) immersed only in BSS (control male vs control female, IMR, p < .05), while such difference was absent between male and female fish immersed in GO (GO male vs. GO female, IMR, p = NS). In contrast to IMR, the number of cells in IRG were found to be identical between the male and female fish injected either with the vehicle or with the GO (vehicle control male vs. vehicle control female, IP, p = NS; GO male vs. GO female, IP, p = NS) (Figure 6A). When the data were compared between the routes of exposure (IMR vs. IP), only the male fish IP-injected with GO (100 μg/g) showed significant decrease in the number of IRG cells compared to male fish exposed to GO by IMR (GO male IMR vs. GO male IP, p < .05) (Figure 6A).

When the HE stained IRG cells are considered separately as DSN and PSN (Figure 6B,C), it appears that both in IMR (20 mg/L, GO) and IP (100 μg/g, GO) fish, only male fish showed significant reduction in DSN cell number compared to corresponding controls (control male vs. GO male, IMR, p < .05; control male vs. GO male, IP, p < .05); in females, GO was found to remain ineffective (control female vs. GO female, IMR, p = NS; control female vs. GO female, IP, p = NS) (Figure 4B). Moreover, gender-specific difference in DSN cell number between males and females of both IMR and IP fish was observed only in control fish (no GO) (control male vs. control female, IMR, p < .05; control male vs. control female, IP, p < .05) and not in fish either immersed (20 mg/L) or IP-injected (100 μg/g) with GO (GO male vs. GO female IMR, p = NS; GO male vs. GO female, IP, p = NS). When the data were compared between the routes of exposure (IMR vs. IP), only the vehicle-injected female control fish (no GO) showed significant decrease in the number of DSN cells compared to male fish immersed only in BSS (control female IMR vs. control female IP, p < .05) (Figure 6B).

In PSN cells, the number in both male and female fish immersed in GO (20 mg/L, IMR), compared to corresponding controls, found to be at the same level (control male vs. GO male, IMR; p = NS; control female vs. GO female, IMR; p = NS) (Figure 6C). Moreover, no gender-specific significant differences between males and females was observed in IMR fish immersed only in BSS (no GO) (control male vs. control female, IMR, p = NS); while significant reduction in PSN cell number was observed in females than males when the fish were immersed in GO (20 m/L) (GO male vs. GO female, IMR; p < .05). In IP fish, compared to corresponding controls, administration of GO (100 μg/g, IP) was able to significantly reduce PSN cell number in females (control females vs. GO females, IP, p < .05) and remained unaltered in males (control male vs. GO male, IP, p = NS) (Figure 6C). Moreover, the number of PSN cells in control (vehicle-injected) females was found to be significantly higher than that of the control males (vehicle control male vs. vehicle control female, IP, p < .05); though this gender-specific difference was absent in fish injected with GO (100 μg/g, IP) (GO male vs. GO female, IP, p = NS).

Using ImageJ software, we were also able to measure the nuclear areas (μm^2) of DSN (Figure 6D) and PSN (Figure 6E) cells of the IMR and IP fish exposed to GO and compared the data with corresponding controls (no GO). The average nuclear areas of DSN and PSN cells of IMR males are 7.246 ± 0.256 μm^2 (n = 36) and 6.993 ± 0.195 μm^2 (n = 59), respectively. However, for IP males the average nuclear areas of DSN and PSN cells are 8.695 ± 0.259 μm^2 (n = 54) and 8.683 ± 0.215 μm^2 (n = 75), respectively. For IMR females, the nuclear areas of DSN and PSN cells are 8.718 ± 0.918 μm^2 (n = 76) and 8.651 ± 0.171 μm^2 (n = 135), respectively. For IP females, the nuclear area of DSN and PSN cells are 8.803 ± 0.25 μm^2 (n = 67) and 8.046 ± 0.166 μm^2 (n = 117), respectively.

Our studies indicate that the DSN cells in male fish immersed in GO (20 mg/L, IMR) or IP-injected (100 μg/g, IP), have significantly

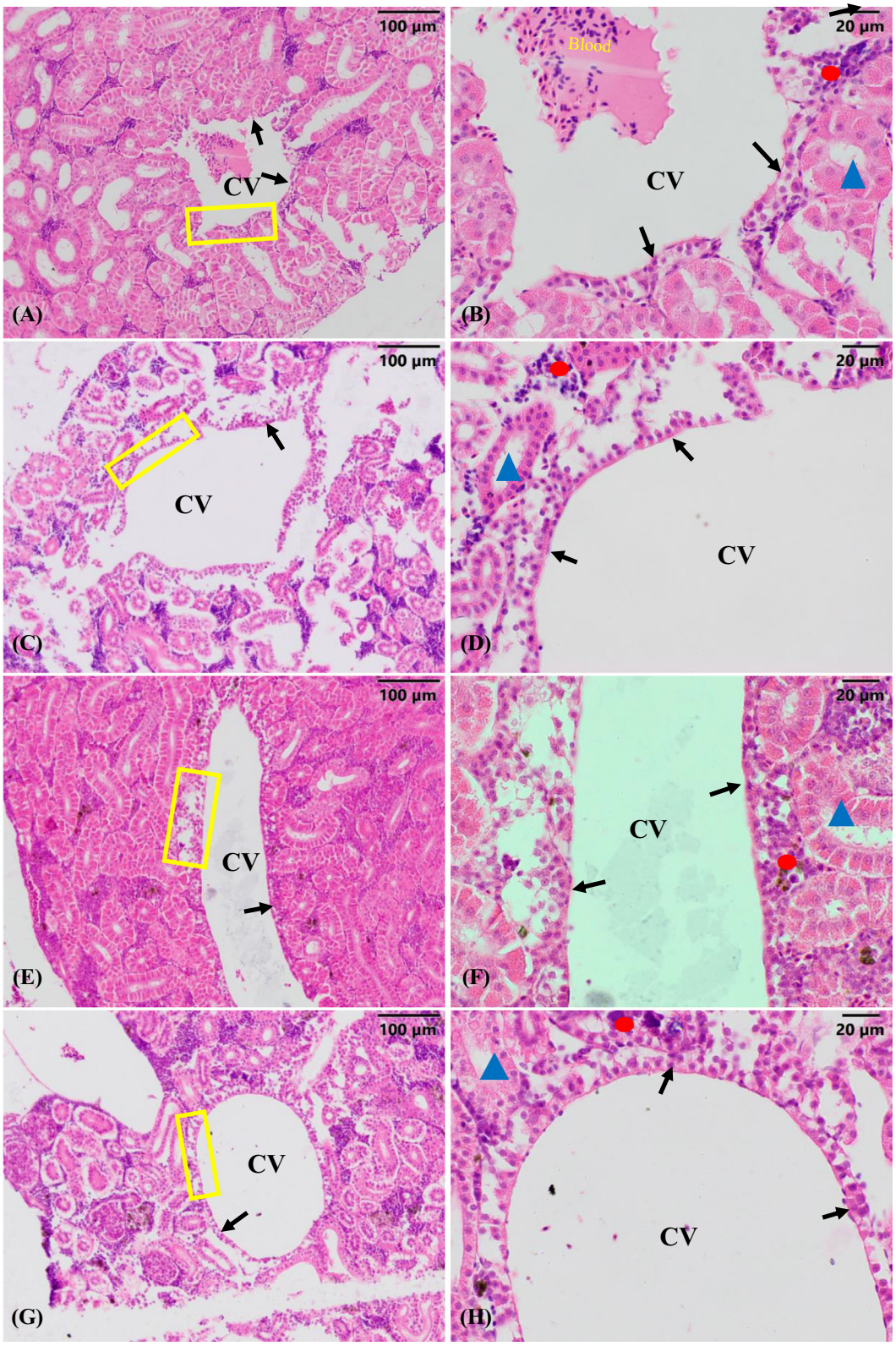

FIGURE 3 Histology of the interrenal gland (IRG) (adrenal homolog) of the adult Japanese medaka exposed to graphene oxide (GO) by IP-injection. Sexually mature and reproductively active adult male and female medaka as breeding pairs were exposed to GO (100 μg/g) by a single IP-injection. Control fish were vehicle-injected with nanopure water. Fish were maintained in BSS for 21 days post-injection in the laboratory condition. IRG was (black arrows) observed adjacent to the posterior cardinal vein (CV) passing through the head kidney. Representative figures are presented as: Figure 3A, IRG of control male fish; Figure 3B, magnified region of the IRG of male fish square marked in Figure 3A; Figure 3C, IRG of control female fish; Figure 3D, magnified region of the IRG of female fish square marked in Figure 3C; Figure 3E, IRG of male fish exposed to GO; Figure 3F, magnified region of the IRG of male fish square marked in Figure 3E; Figure 3G, IRG of female fish exposed to GO; Figure 3H, magnified region of the IRG of female fish square marked in Figure 3G; black arrow, IRG; blue triangle: renal tubule (renal unit of the kidney): red circle: interstitial cells (immune unit of the kidney).

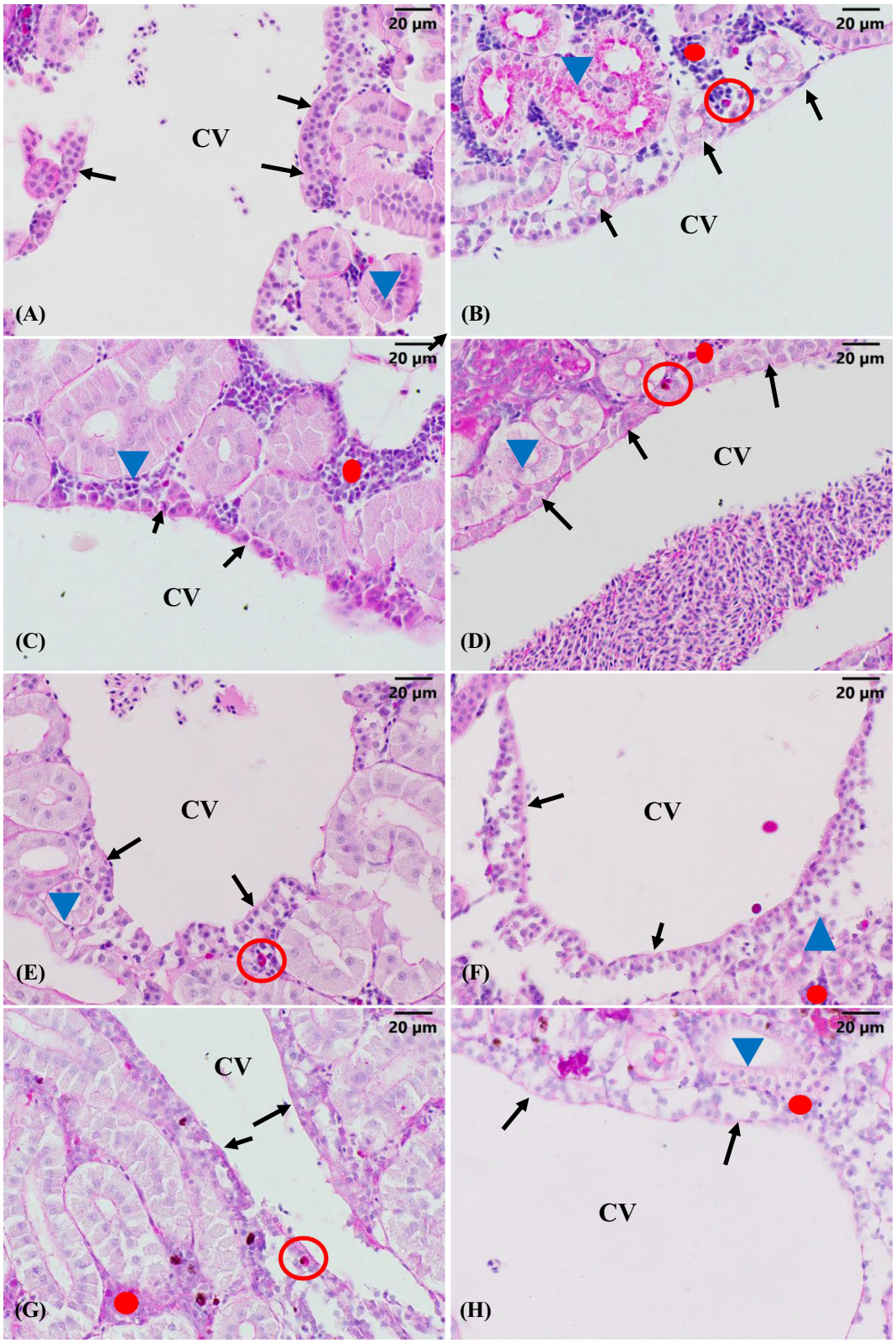

FIGURE 4 Representative photomicrographs of histochemical evaluation of the interrenal gland (IRG) of medaka adults. Histochemical studies were conducted by periodic acid-Schiff reactions (PAS). Sexually mature and reproductively active adult male (Figure 4A, C, E, and G) and female (Figure 4B, D, G, and H) medaka as breeding pairs were exposed to graphene oxide (GO) either by immersion (20 mg/L) (Figure 4C,D) or by a single IP- injection (100 μg/g) (Figure 4G,H). Parallel controls were either immersed in balanced salt solution (Figure 4A,C) or vehicle-injected (Figure 4E,F) with no GO. PAS reactivity of the IRG cells was evaluated after 21 days post-treatment. The cells (IRG cells; marked by black arrows) are PAS negative, however, in a few cases, the cytoplasm appears to pink-red (Figure 4C). PAS positive regions in the renal units of kidneys are cilia of proximal tubules; however in immune units, the melanomacrophages due to lipofuscin are PAS positive (appears red within open red circles). In a few cases, PAS positive melanomacrophages are found to be associated with the IRG (Figure 4D,G). CV, cardinal vein; black arrow, IRG; blue triangle: renal tubule (renal unit of the kidney); filled red circle: interstitial cells (immune unit of the kidney).

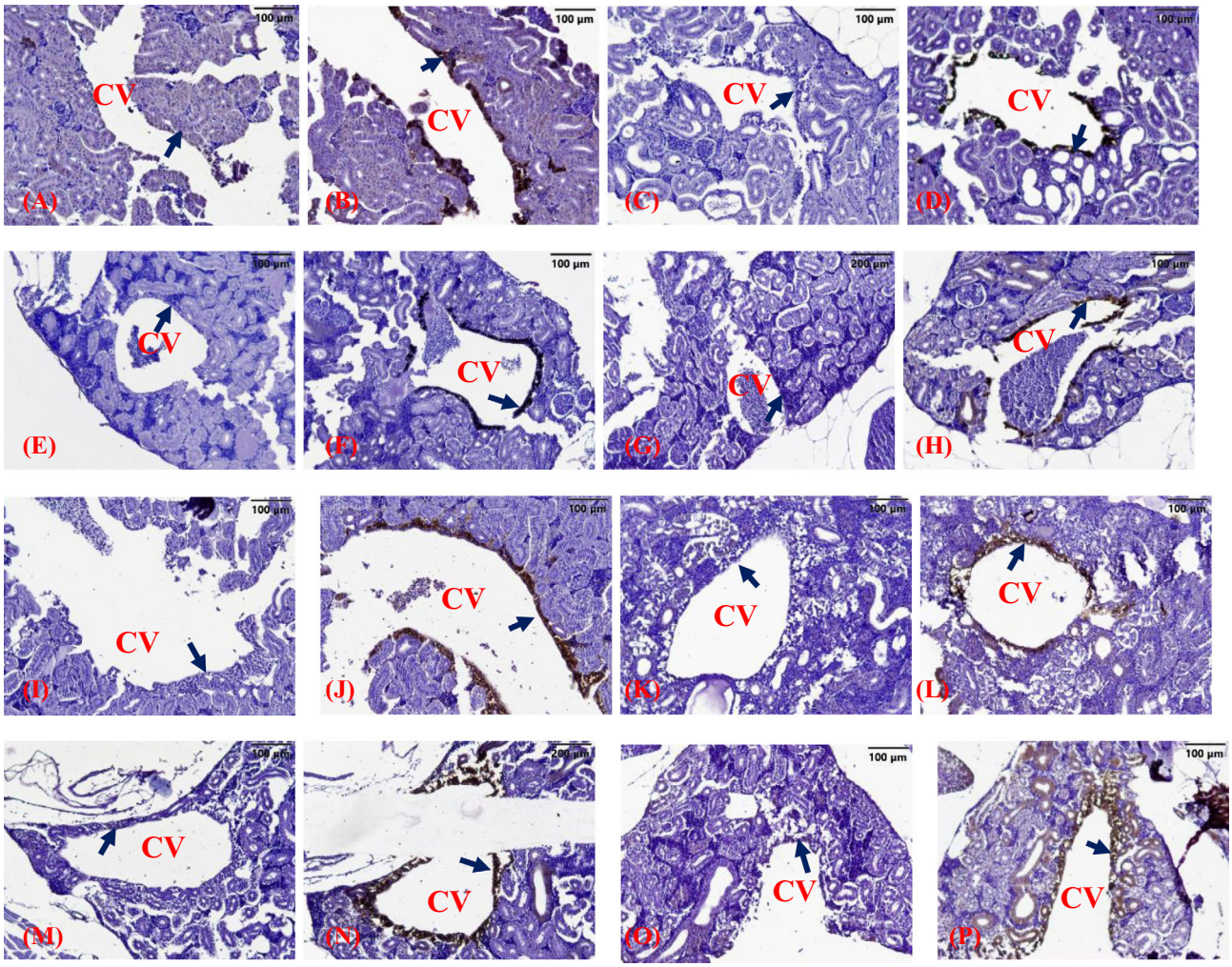

FIGURE 5 Immunohistochemical localization of the tyrosine hydroxylase enzyme on of the interrenal gland (IRG) (adrenal homolog) of the adult Japanese medaka exposed to graphene oxide (GO). Representative figures are presented as: Figure 5A, immunostaining of the IRG of control immersion (IMR) male fish without primary antibody; Figure 5B, immunostaining of the IRG of the same control IMR male fish (Figure 5A) with primary antibody; Figure 5C, immunostaining of the IRG of male fish exposed to GO (20 mg/L) by IMR without primary antibody; Figure 5D: immunostaining of the IRG of the same male fish (Figure 5C) exposed to GO (20 mg/L) by IMR with primary antibody; Figure 5E, immunostaining of the IRG of control IMR female fish without primary antibody; Figure 5F, immunostaining of the IRG of control IMR same female fish (Figure 5E) with primary antibody; Figure 5G, immunostaining of the IRG of female fish exposed to GO (20 mg/L) by IMR without primary antibody; Figure 5H, immunostaining of the IRG of the same female fish (Figure 5G) exposed to GO (20 mg/L) by IMR with primary antibody; Figure 5I, immunostaining of the IRG of control IP male fish without primary antibody; Figure 5J, immunostaining of the IRG of the same control IP male fish (Figure 5I) with primary antibody; Figure 5K, immunostaining of the IRG of GO- injected (100 μg/g) male fish without primary antibody; Figure 5L, immunostaining of the IRG of GO- injected (100 μg/g) same male fish (Figure 5K) with primary antibody; Figure 5M, immunostaining of the IRG of IP-injected control female fish without primary antibody; Figure 5N, immunostaining of the IRG of GO- injected (100 μg/g) same male fish (Figure 5M) with primary antibody; Figure 5O, immunostaining of the IRG of female fish exposed to GO (100 μg/g) by IP without primary antibody; Figure 5P, immunostaining of the IRG of the same female fish (Figure 5O) exposed to GO (100 μg/g) by IP with primary antibody; CV, cardinal vein; black arrow, IRG.

higher nuclear areas (hypertrophy) than the corresponding control males (control male vs. GO male, IMR, $p < .05$; control male vs. GO male, IP, $p < .05$); however, in females, significant hypertrophy was observed only in fish immersed in GO (20 mg/L, IMR), and remained unaltered in fish administered GO (100 μg/g, IP) (control female vs. GO females, IMR, $p < .05$; vehicle control female vs. GO females, IP, $p =$ NS) (Figure 4D). Moreover, compared to males, gender-specific nuclear hypertrophy was observed in DSN cells of females, immersed only in BSS, however, such hypertrophy (gender-specific) was absent between male and female fish when immersed in GO (control male vs. control females, IMR, $p < .05$; GO male vs. GO female, IMR, $p =$ NS). In contrast to IMR, gender-specific hypertrophy of the nuclear area of DSN cells was observed in female fish injected-IP with GO (100 μg/g, IP) (GO male vs. GO female, IP, $p < .05$), absent in fish injected with vehicle only (control) (vehicle control male vs. vehicle control female, IP, $p =$ NS) (Figure 6D). When the data were

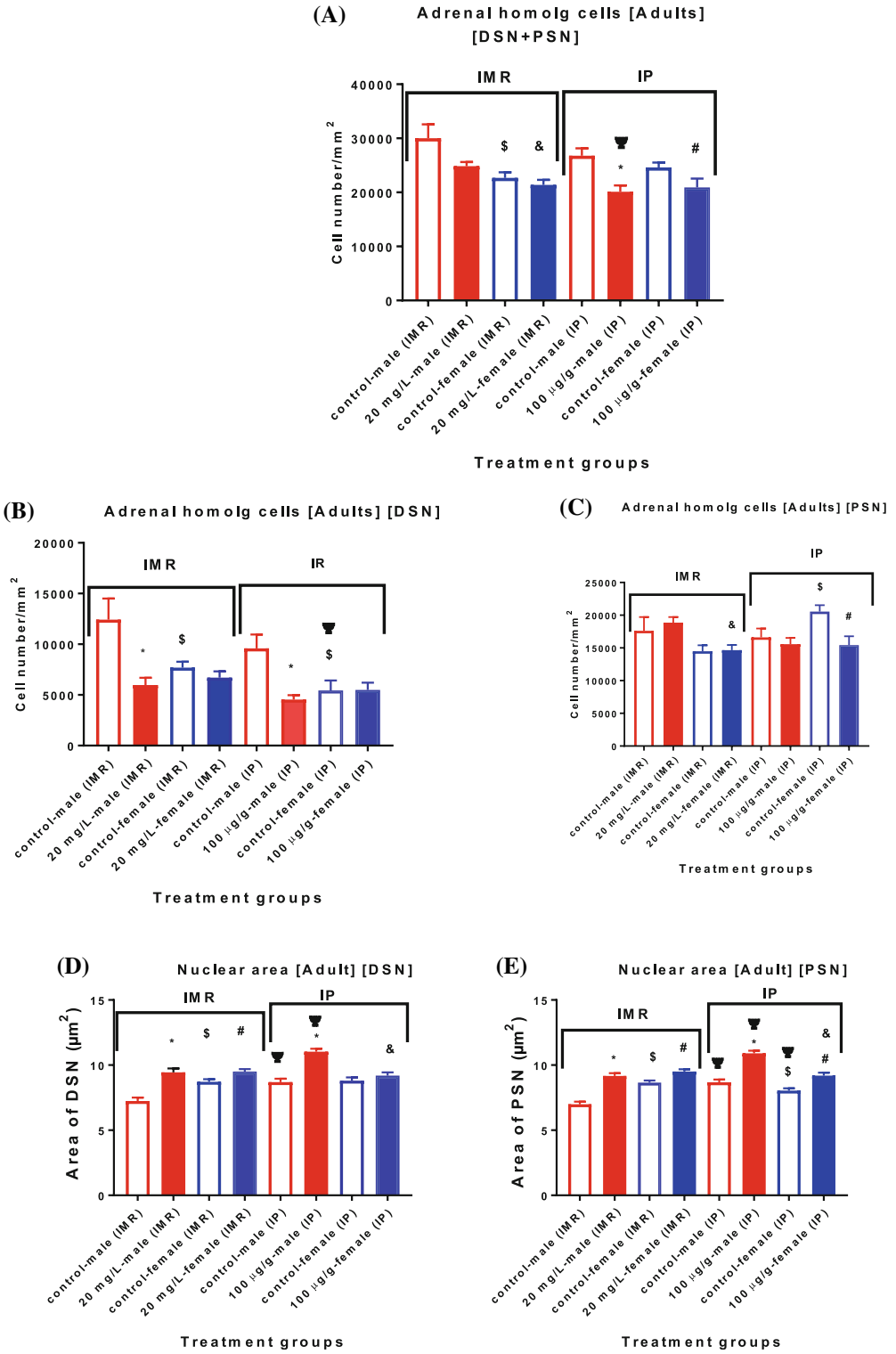

FIGURE 6 Distribution of interrenal gland (IRG) (adrenal homolog) cells and the nuclear area of IRG cells in Japanese medaka adults after graphene oxide (GO) exposure. Reproductively active adult male and female Japanese medaka as breeding pairs were exposed to GO either by immersion (IMR) at the concentration of 20 mg/L continuously for 96 h in balanced salt solution or by intraperitoneal injection (IP) at the dose of 100 µg/g. Controls in IMR experiment were maintained in BSS only and for IP experiments were vehicle-injected (nanopure water) and maintained in BSS. The fish, after GO treatment were maintained in a GO-free environment in the laboratory for 21 days and sacrificed for histological evaluation of the IRG cells stained in HE. Each bar represents the mean ± *SEM*. The bar heads with asterisks (*) represent significant difference between control males (IMR or IP) with the corresponding males exposed to GO either by IMR or IP, respectively. Pound symbol (#) indicate significant difference between control IMR or IP females with corresponding IMR (20 mg/L) or IP (100 µg/g) females exposed to GO. Dollar symbol ($) indicate significant difference between the male and female fish exposed as controls or treated with GO by IMR. Symbol "&" indicate significant difference between the male and female fish exposed to GO by IP. Greek letter "Ψ" indicate significant different between the route of exposures of fish (either male or female) exposed to GO or control by IMR and IP. IMR, the experimental fish immersed in BSS either as control or with 20 mg/L GO. IP, the experimental fish intraperitoneally-injected either vehicle (control) or GO (100 µg/g) and maintained in BSS.

compared between the routes of exposure (IMR vs. IP), the vehicle-injected IP control male fish showed significant hypertrophy in the nuclear area of DSN cells compared to male fish immersed only in BSS (control male IMR vs. control male IP, $p < .05$); moreover, the male fish IP-injected with GO (100 μg/g) also showed significant nuclear hypertrophy in DSN cells than the male fish immersed in GO (20 mg/L) (GO male IMR vs. GO male IP, $p < .05$) (Figure 6D). In contrast to males, females either as control or exposed to GO by IMR and IP, did not show any significant difference in the nuclear area of DSN cells (GO female IMR vs. GO female IP, p = NS; GO female IMR vs. GO female IP, p = NS) (Figure 6D). In PSN cells, like DSN, the nuclear area in both male and female fish exposed to GO either by IMR (20 mg/L) or through IP-administration (100 μg/g, IP), induced significant nuclear hypertrophy compared to the corresponding control male and female fish (either immersed in BSS or vehicle-injected) (control male vs. GO male, IMR, $p < .05$; control female vs. GO female, IMR, $p < .05$; vehicle control male vs. GO male, IP, $p < .05$; vehicle control female vs. GO female, IP, $p < .05$) (Figure 6E). Moreover, gender-specific nuclear hypertrophy was also observed in PSN cells of females immersed only in BSS (control male vs. control female, IMR, $p < .05$), not in fish exposed to GO (20 mg/L, IMR) (GO male vs. GO female, IMR, p = NS). However, in IP fish, nuclear hypotrophy in females was observed in both vehicle-injected (control) as well as in GO-injected fish (100 μg/g, IP) (vehicle control male vs. vehicle control female, IP, $p < .05$; GO male vs. GO female, IP, $p < .05$) (Figure 6E). When the data were compared between the routes of exposure (IMR vs. IP), the vehicle-injected IP control male or female fish showed a significant nuclear hypertrophy in PSN cells compared to male or female fish immersed only in BSS (control male IMR vs. control male IP, $p < .05$; control female IMR vs. control female IP, $p < .05$); moreover, the male fish IP-injected with GO (100 μg/g) also showed a significant nuclear hypertrophy in PSN cells than the male fish immersed in GO (20 mg/L) (GO male IMR vs. GO male IP, $p < .05$) (Figure 6E). In contrast to males, females exposed to GO by IMR, did not show any significant differences in the nuclear area of PSN cells of females injected-IP with GO (GO female IMR vs. GO female IP, p = NS) (Figure 6E).

3.3 | Effect of GO exposure on larvae

The morphological observations of the IRG of the Japanese medaka larvae (male and female phenotypes as well as XY and XX genotypes) on 47th dph by light microscopy after HE (Figure 7) or PAS (Figure 8) and immunostaining (Figure 9) appear to be identical with the features we have observed in adult male or female medaka (Figures 2–5). In brief, the cells were arranged either as a single, or in groups, with occasional encircling a sinusoid, or as a straight cord, near the endothelium of the cardinal vein passing through the cephalic kidney (Figure 7). The shape of the cells appeared to be columnar or oval, and were in contact either with the hematopoietic tissue or separated from it by the sinusoids. Histochemically, the IR axis cells, were found to be negative for PAS (Figure 8). Moreover, immunohistochemical studies also indicated that the IRG of medaka larvae possess TH-immunoreactive cells as observed in adults (Figure 9).

Furthermore, the histological (Figure 7), histochemical (Figure 8), and immunohistochemical evaluation (Figure 9) of the of the IRG of the Japanese medaka larvae exposed to different concentrations of GO by IMR (2.5–20 mg/L; 96 h continuous; Figures 7–9) were done after 6 weeks of depuration in a GO-free environment. We have observed that the morphological features of the IRG of the larvae of both male (testis) (Figure 7B,D) and female (ovary) phenotypes (Figure 7F) or male (XY) (Figure 7B) and female (XX) genotypes (Figure 7D,F), exposed to GO (20 mg/L), were found to be almost identical with the corresponding control male (testis) (Figure 7A,C) and female (ovary) phenotypes (Figure 7E) or male (XY) (Figure 7A) and female (XX) genotypes (Figure 7C,E). Histochemical (PAS) and immunohistochemical (TH) evaluation did not show any apparent effect of GO on the IRG cells in the male (Figures 8B,F and 9C–H) or female phenotypes (Figures 8D,E and 9A,B) as well as in male (XY) (Figure 8B and 9C–F) and female (XX) genotypes (Figures 8D–F and 9A,B,G,H), however, the cilia of proximal tubules (renal units) and the melanomacphage in the lymphyomyeloid regions of the kidney were found to be PAS positive (Figure 8).

3.4 | Distribution of IRG cells of Japanese medaka larvae exposed to GO by IMR

Like adults, we have counted the IRG cells in different regions of the IRG of Japanese medaka larvae irrespective of the nuclear staining intensity (DSN + PSN) and expressed as number of cells/mm^2 area of IRG (Figure 10). The average number of IRG cells in medaka larvae, we were able to count in controls having male genotypes (XY) are 41 305 ± 1654 cells/mm^2 (n = 20) and 29 498 ± 2562 cells/mm^2 (n = 17) for female genotypes (XX). Similarly, in control male (testis) and female (ovary) phenotypes the number is 38555 ± 1949/mm^2 (n = 25) and 30 294 ± 3106 cells/mm^2 (n = 12), respectively. In both cases (genotypes and phenotypes), the data (XY vs. XX and testis vs. ovary) are significantly different and the males either as genotypes (XY) or phenotypes (testis) have significantly higher number of cells/mm^2 than the corresponding female genotypes (XX) or phenotypes (ovary) ($p < .05$) (Figure 10A,B).

Our data indicated that the IRG cells in the larvae of males genotypes (XY) showed significant reduction in 2.5 and 20.0 mg/L group when compared with controls, however, other groups (5 and 10.0 mg/L) did not show any significant effects (Figure 10A). Intergroup comparisons between different GO-exposed larvae (2.5–20 mg/L) indicated significantly higher number of IRG cells in 5–20 mg/L groups than only with 2.5 mg/L group. In female genotypes (XX), the larvae exposed to different concentrations of GO (2.5–20.0 mg/L) did not show any significant difference in IRG cell numbers when compared with controls (no GO). Moreover, intergroup comparison within the larvae exposed to different GO groups did not show any significant concentration-dependent effects. However, like controls (no GO), sex-specific differences between genotypic males

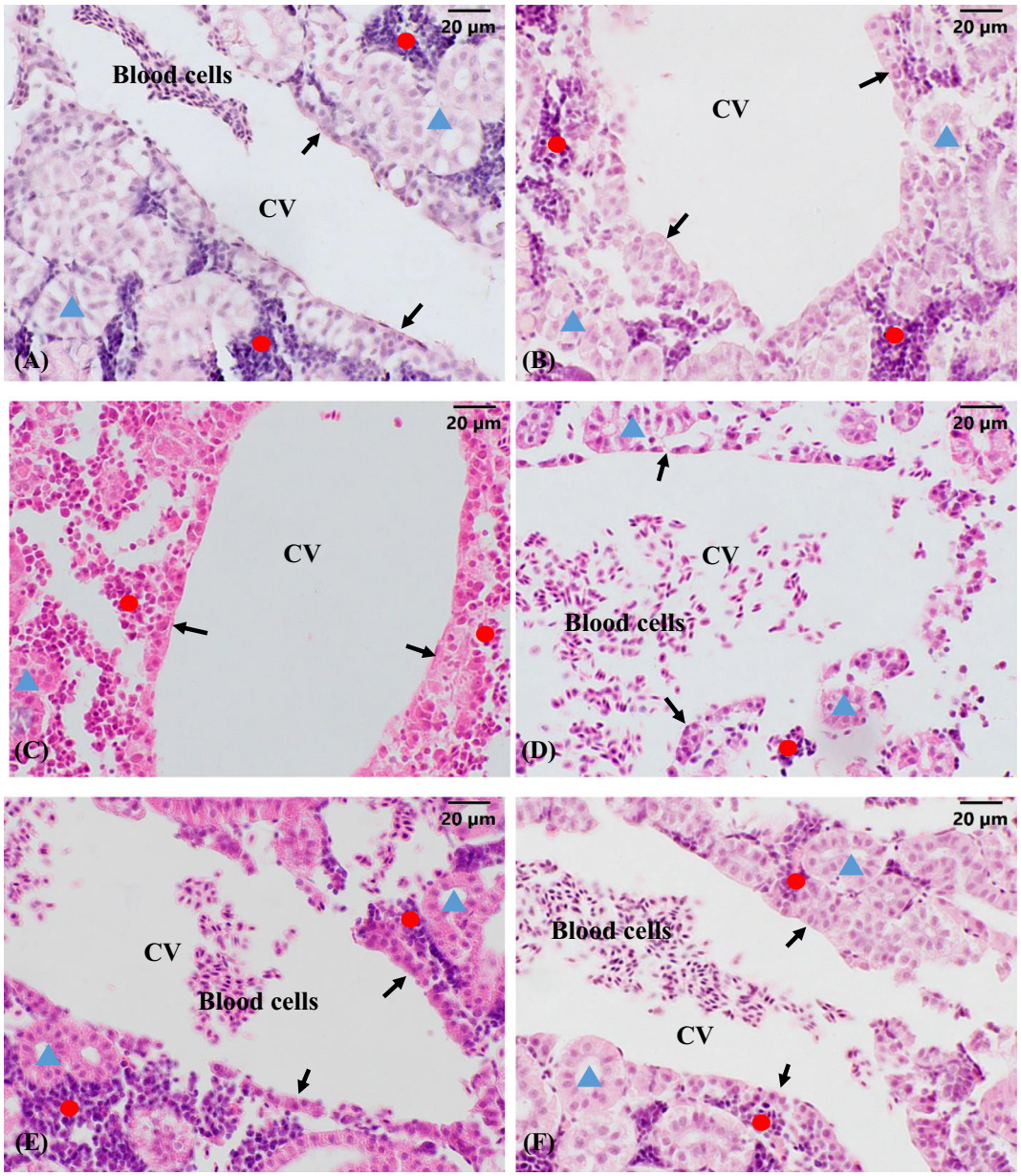

FIGURE 7 Effect of graphene oxide (GO) exposure on the histology of the interrenal gland (IRG) (adrenal homolog) of Japanese medaka larvae. 1 day post-hatch Japanese medaka larvae were exposed to GO (2.5–20 mg/L) in embryo rearing medium continuously for 96 h and then maintained in balanced salt solution (no GO) for 6 weeks. Control larvae were maintained in identical condition with no GO. IRG are (black arrows) observed adjacent to the posterior cardinal vein (CV) passing through the head kidney. Representative HE figures (control and 20 mg/L GO) are presented as: Figure 7A, IRG of control male phenotype (testis) and male genotype (XY); Figure 7B, IRG of male phenotype (testis) and male genotype (XY) exposed to 20 mg/L GO; Figure 7C, IRG of control male phenotype (testis) and female genotype (XX); Figure 7D, IRG of male phenotype (testis) and female genotype (XX) exposed to 20 mg/L GO; Figure 7E, IRG of control female phenotype (ovary) and female genotypes (XX); Figure 7F, IRG of female phenotype (ovary) and female genotype (XX) exposed to 20 mg/L GO. CV, cardinal vein; black arrow, IRG; blue triangle: renal tubule (renal unit of the kidney); red circle: interstitial cells (lymphoid and hematopoietic units of the kidney).

(XY) and females (XX) were observed in some of the larvae exposed to equal concentrations GO (Figure 10A). Larvae with female genotypes (XX) exposed to 2.5 mg/L GO have significantly higher number of IRG cells than males (XY) exposed to 2.5 mg/L, while the larvae (female XX) exposed to 5.0 mg/L have significantly reduced number of cells than males (XY) exposed to identical GO concentrations (5.0 mg/L). In other test concentrations (10–20 mg/L), GO did not show any significant sex-specific effects between the male (XY) and female (XX) genotypes (Figure 10A).

In contrast to genotypes, male phenotypes (testis) exposed to different concentrations of GO (2.5–20 mg/L) showed significant reduction in IRG cell number (/mm^2) only in 2.5 and 5.0 mg/L groups than controls (Figure 10B); moreover, other groups (5–20 mg/L) did not show any significant difference in IRG cell number with controls.

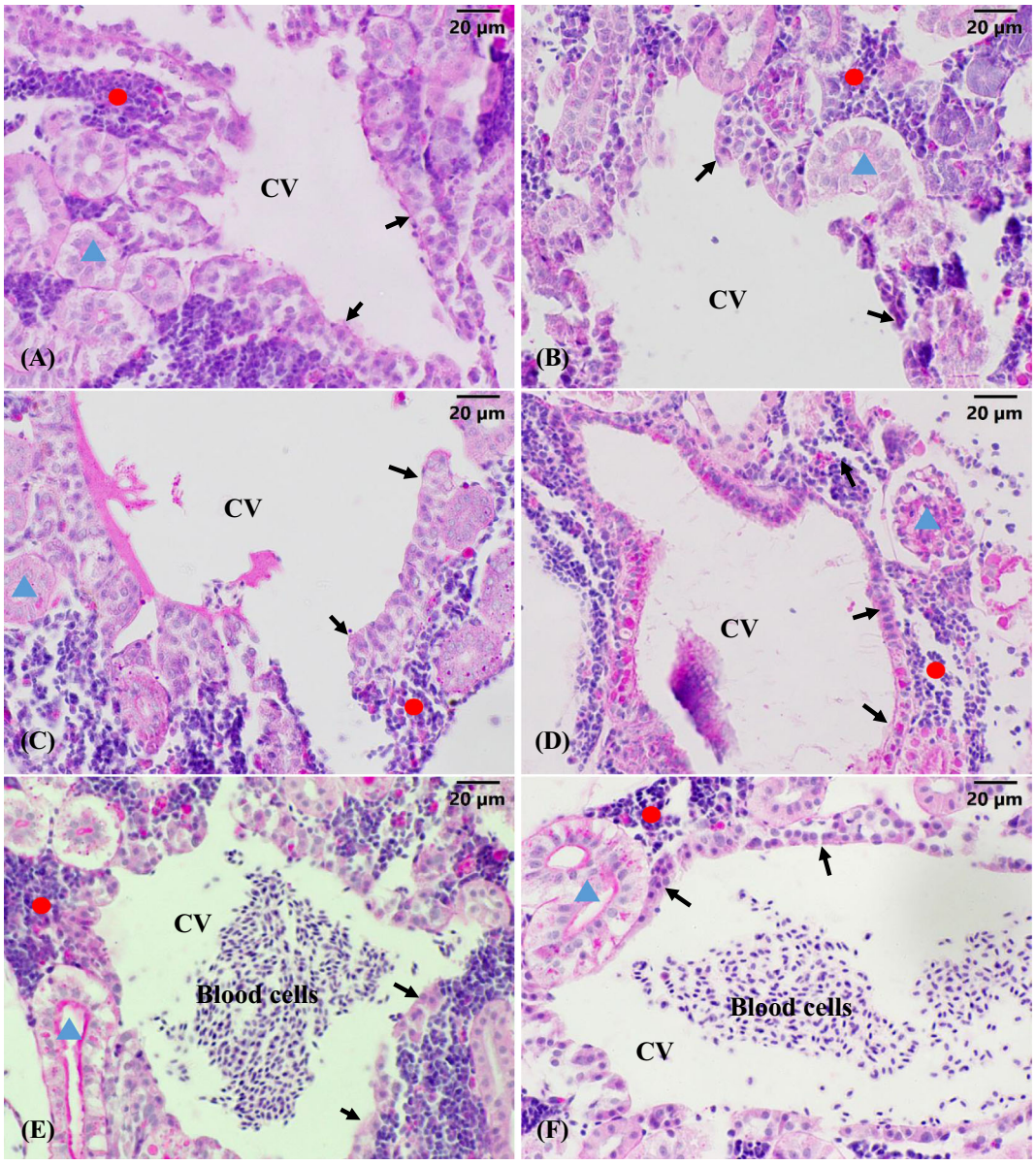

FIGURE 8 Representative photomicrographs of histochemical evaluation of the interrenal gland (IRG) of medaka larvae. 1 day post-hatch Japanese medaka larvae were exposed to graphene oxide (GO) (2.5–20 mg/L) in embryo rearing medium continuously for 96 h and then maintained in balanced salt solution (no GO) for 6 weeks. Control larvae were maintained in identical condition with no GO. Histochemical studies were conducted by periodic acid-Schiff (PAS) reactions. PAS reactivity of the IRG cells was evaluated after 6-weeks post-treatment. The cells (IRG cells; marked by black arrows) are PAS negative. PAS positive regions in the renal units of kidneys are cilia of proximal tubules; however in immune units, the melanomacrophages due to lipofuscin are PAS positive. CV, cardinal vein; black arrow, IRG; blue triangle: renal tubule (renal unit of the kidney); red circle: interstitial cells (lymphoid and hematopoietic units of the kidney) Figure 8A, control male phenotype (testis) and male genotype (XY); Figure 8B, male phenotype (testis) and male genotype (XY) exposed to 20 mg/L GO; Figure 8C, control female phenotype (ovary) and female genotype (XX); 8D, female phenotype (ovary) and female genotype (XX) exposed to 20 mg/L GO; Figure 8E, female phenotype (ovary) and female genotype (XX) larva exposed to 2.5 mg/L GO; Figure 8F, Male phenotype (testis) and female genotype (XX) larva exposed to 20 mg/L GO.

When comparisons were made between different concentrations of GO, only 2.5 and 5.0 mg/L groups showed significantly reduced number of cells compared to the 10 and 20 mg/L groups (Figure 10B). In female phenotypes (ovary), like genotypes (XX), no significant effect on IRG cell numbers was observed in any of the GO exposed groups (2.5–20 mg/L) when compared with the corresponding controls or within the different GO concentrations groups (Figure 10B). However, in contrast to controls (no GO), female phenotypes (ovary) exposed to 2.5 mg/L GO, showed significantly higher number of IRG cells than male phenotypes (testis) exposed to equivalent GO concentration (2.5 mg/L), while other larvae exposed to higher concentrations of GO (5–20 mg/L) were unable to establish significant sex-specific

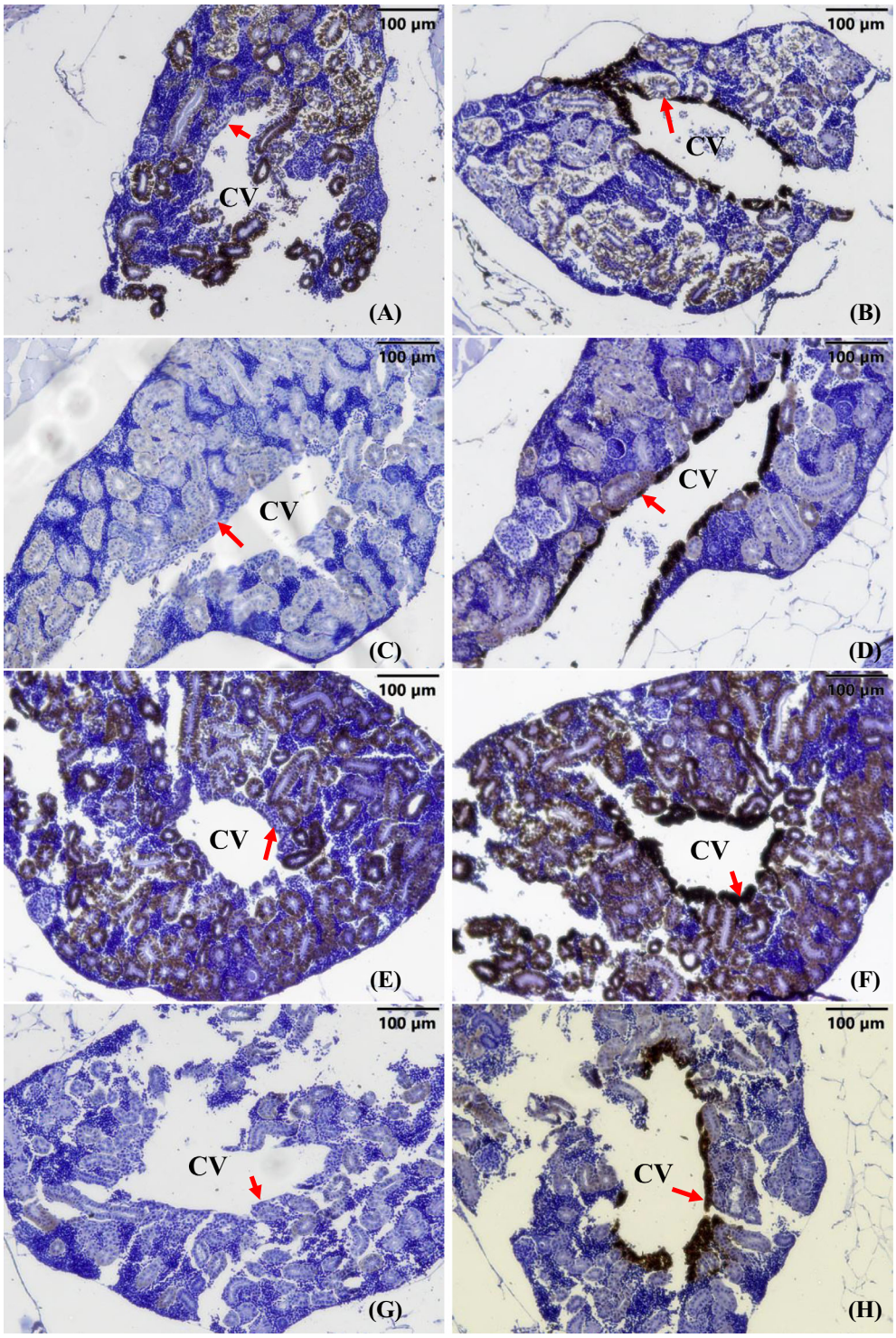

FIGURE 9 Immunohistochemical localization of the Tyrosine hydroxylase enzyme on of the interrenal gland (IRG) (adrenal homolog) of the Japanese medaka larvae exposed to graphene oxide (GO) by immersion. Representative figures are presented as: Figure 9A, Immunostaining of the IRG of control female larvae (phenotypic ovary with XX genotype) without primary antibody; Figure 9B, Immunostaining of the IRG of same larva (Figure 9A) with primary antibody. Although we are unable to avoid background reaction on renal tubules, the IRG adjacent to cardinal vein are negative in Figure 9A and positive in Figure 9B (marked by red arrows); Figure 9C, Immunostaining of the IRG of a male (testis with XY genotype) larvae exposed 20 mg/L GO during first fry stage without primary antibody; Figure 9D, Immunostaining of the IRG of the same male (Figure 9C) larvae exposed 20 mg/L GO during first fry stage with primary antibody; Figure 9E, Immunostaining of the IRG of a male (testis with XY genotype) larva exposed to 10 mg/L GO during first fry stage without primary antibody; Figure 9F, Immunostaining of the IRG of the same male (Figure 9E) larva exposed to 10 mg/L GO during first fry stage with primary antibody; Figure 9G, Immunostaining of the IRG of a male (testis with XX genotype) larvae exposed to 5.0 mg/L GO during first fry stage without primary antibody; Figure 9H, Immunostaining of the IRG of the same male (Figure 9G) larvae exposed to 5.0 mg/L GO during first fry stage with primary antibody. CV, cardinal vein; red arrow, IRG.

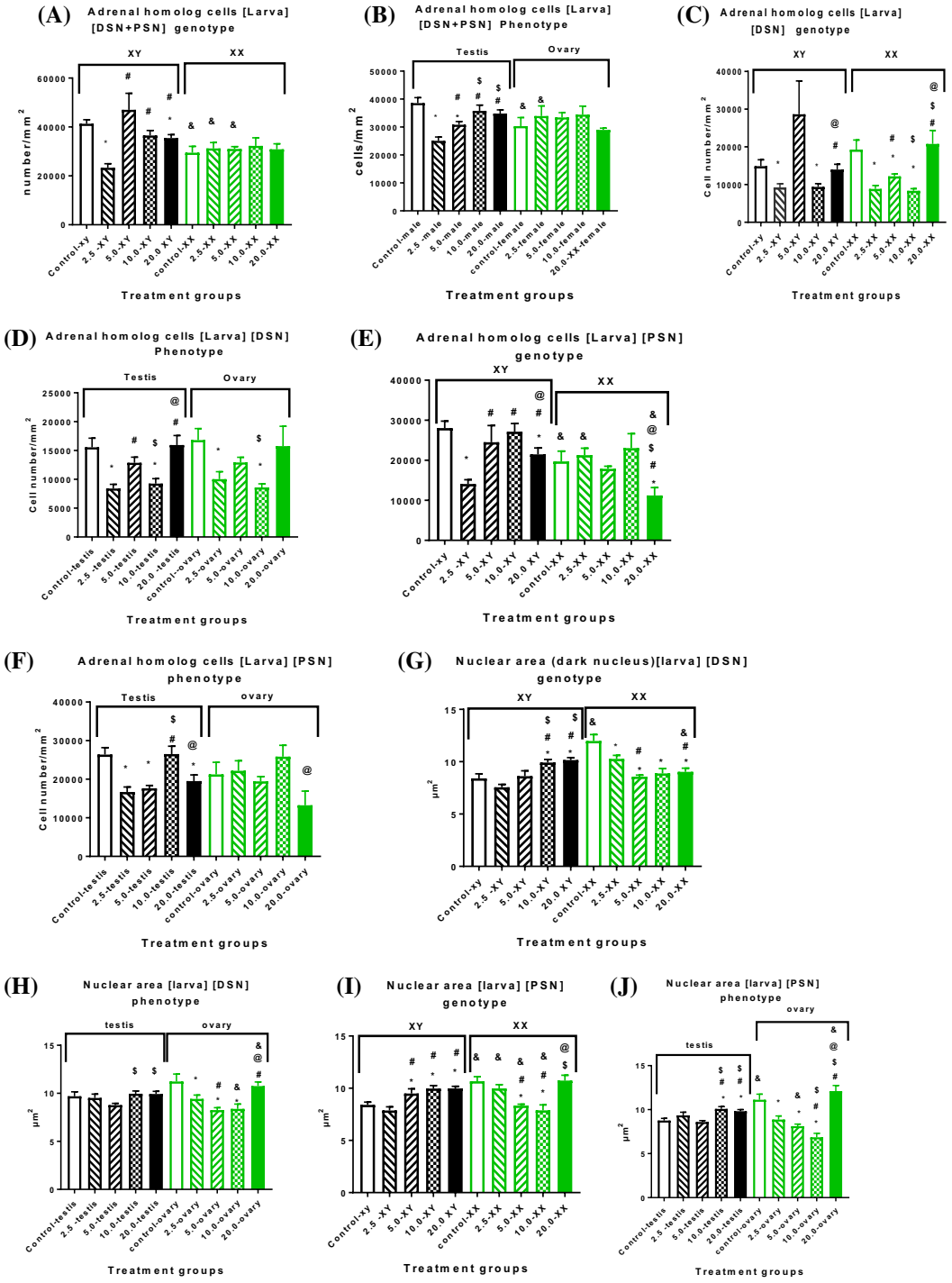

FIGURE 10 Distribution of interrenal gland (IRG) (adrenal homolog) cells (either as total cells or as deep-stained nuclei [DSN] or pale-stained nuclei [PSN] cells) and the nuclear area (DSN and PSN cells) in Japanese medaka larvae after graphene oxide exposure. 1 day post-hatch Japanese medaka larvae were exposed to GO (2.5–20 mg/L) in embryo rearing medium by immersion continuously for 96 h and then maintained in balanced salt solution (no GO) for 6 weeks. Each bar represent the mean ± *SEM*. The bar heads with asterisks (*) represent that the data are significantly different ($p < .05$) from control genotypes (XY or XX) or phenotypes (testis or ovary). The pound symbol (#) indicate significant difference with genotypic (XY or XX) or phenotypic (testis or ovary) larvae exposed to 2.5 mg/L GO; dollar symbol ($) indicate significant difference with genotypic (XY or XX) or phenotypic (testis or ovary) larvae exposed to 5.0 m/L GO. Symbol @ indicate significant difference with the genotypic (XY or XX) or phenotypic (testis or ovary) larvae exposed to 10 mg/L GO. The symbol & indicate significant difference between genotypes (XY and XX) or phenotypes (testis and ovary) having identical exposure conditions (between the genotypes and phenotypes of controls or between the genotypes and phenotypes of the larvae exposed to the identical GO concentrations).

differences between male and female phenotypes as observed in 2.5 mg/L (Figure 10B).

Furthermore, we have also separated the IRG cells of medaka larvae into DSN (Figure 10C,D) and PSN (Figure 10E,F) cell types. The DSN cells in the IRG of control male and female genotypes (XY and XX) are remained at the same level (Figure 10C) as in control male (testis) and female (ovary) phenotypes (Figure 10D). The effects of GO in both male (XY) and female (XX) genotypes indicated that, compared to controls, in males (XY), GO at 2.5 and 10 mg/L concentrations significantly reduced the number of DSN cells in the IRG, however, both 5.0 and 20.0 mg/L did not show any significant effects (Figure 10C). Further comparisons of the data within the different concentrations of GO (2.5–20 mg/L), did not show any consistent concentration-dependent effects in males (XY), while the larvae exposed to 20 mg/L showed concentration-dependent enhancement in DSN cell numbers compared to 2.5 and 10.0 mg/L groups (Figure 10C). In females (XX), GO at 2.5–10 mg/L concentrations, were able to significantly reduced DSN cells when compared with controls (XX), however, no significant difference in controls was observed in larvae exposed to 20.0 mg/L (Figure 10C). Comparison of the larvae exposed to different GO concentrations (2.5–20 mg/L) indicated a concentration-dependent enhancement in larvae exposed to 5.0 and 20.0 mg/L, compared to the larvae (XX) exposed to 2.5 mg/L GO, however, the larvae exposed to 10.0 mg/L showed significant decrease in comparison to the larvae exposed to 5.0 mg/L GO (Figure 10C). The effects of GO in male (testis) and female (ovary) phenotypes indicated that in males (testis), GO at the concentrations of 2.5 and 10 mg/L, compared to controls (no GO), were able to significantly reduce the DSN cell numbers in the IRG of larvae, while in other concentrations (5 and 20 mg/L) the cell number remained unaltered (Figure 10D). Moreover, comparison of the data (DSN cell number/mm^2) within the different concentrations of GO (2.5–20 mg/L) did not show any consistent effects. The larvae (testis) exposed to 5.0 and 20.0 mg/L GO had significantly higher number of cells than the larvae exposed to 2.5 mg/L GO, while the DSN cells in 5.0 mg/L larvae were found to be significantly higher than the larvae exposed to 10.0 mg/L. Moreover, male phenotypes (testis) with 20.0 mg/L GO have significantly higher number of DSN cells than 10.0 mg/L GO (Figure 10D). In females (ovary), GO at 2.5 and 10.0 mg/L concentrations were able to significantly reduced the DSN cells in the IRG of larvae, while other two concentrations (5.0 and 20.0 mg/L) did not show any significant difference (Figure 10D). Comparison of the data within the female phenotypes (ovary) exposed to different concentrations of GO (2.5–20 mg/L) indicated only significant reduction in 10.0 mg/L groups when compared with 5.0 mg/L groups. Moreover, as observed in control larvae, sex-specific differences in DSN cells between male (XY) and female (XX) genotypes as well as between male (testis) and female (ovary) phenotypes maintained in identical GO concentrations (2.5–20) were found to be absent (Figure 10C,D).

The PSN cells in control larvae having male genotypes (XY), showed significantly higher number of cells than females (XY) (Figure 10E), while the male (testis) and female (ovary) phenotypes did not show any significant differences (Figure 10F). Further, comparison within male (XY) genotypes indicated that, compared to controls, the number of PSN cells were reduced significantly in larvae exposed to 2.5 and 20.0 mg/L GO (Figure 10F). Moreover, males (XY) exposed to different concentrations of GO (2.5–20.0 mg/L) indicated that, compared to 2.5 mg/L group, the PSN cell number were significantly increased in the larvae exposed to 5.0–20.0 mg/L GO, however, the larvae (XY) in 20.0 mg/L group showed significant reduction in PSN cell number when compared with only 10.0 mg/L group. In females (XX), compared to controls, significant reduction in PSN cell number was observed in larvae exposed only in 20 mg/L GO, while other groups (2.5–10.0 mg/L) did not show any significant difference (Figure 10E). Comparison of the PSN cell number between the larvae exposed to different concentrations of GO indicated that only the larvae exposed to 20 mg/L GO showed significant reduction in comparison with all other GO-exposed groups (2.5–10.0 mg/L). For sex-specific differences between male (XY) and female (XX) genotypes exposed to GO (2.5–20.0 mg/L) indicated that, in contrast to controls, significant reduction in PSN cell number was observed in females (XX) maintained either in 2.5 or 20.0 mg/L GO. Other female (XX) groups (5.0 and 10.0 mg/L GO) maintained equal PSN cell status as in male genotypes (XY) (Figure 10F). Further, in male phenotypes (testis), the larvae exposed to 2.5,5, and 20 mg/L GO showed significant reduction, while in females (ovary), GO (2.5–20 mg/L) was unable to significantly alter the PSN cell populations in IRG when compared with the corresponding controls (Figure 10F). Further comparison of the PSN cell number within the different GO exposed groups indicated significant increase in PSN cell number in males (testis) exposed to 10.0 mg/L GO when compared with 2.5 and 5.0 mg/L GO groups. Moreover, significant reduction in PSN cell number was observed in males (testes) exposed to 20.0 mg/L GO than the larvae in 10.0 mg/L. In females (ovary), 2.5, 5.0, and 10.0 mg/L maintained equal status except 20 mg/L where significant reduction in PSN cell number was observed when compared only with 10.0 mg/L GO groups. Moreover, like controls, sex-specific effects of GO (2.5–20.0 mg/L) between phenotypic males (testis) and females (ovary) was found to be absent in the larvae maintained in any of the GO concentrations (Figure 10F).

Like adults, we have also measured the area (μm^2) of the nuclei of DSN (Figure 10G,H) and PSN (Figure 10I,J) cells in larvae exposed to different concentrations of GO (2.5–20 mg/L) and compared the data with corresponding control (no GO) male (XY) and female (XX) genotypes as well as between control male (testis) and female (ovary) phenotypes. Our data indicated that the average nuclear areas of DSN cells in control male (XY) and female (XX) genotypes are 8.41 ± 0.44 μm^2 ($n = 48$) and 11.98 ± 0.62 μm^2 ($n = 47$), while in control male (testis) and female (ovary) phenotypes are 9.69 ± 0.46 μm^2 ($n = 63$) and 9.42 ± 0.40 μm^2 ($n = 27$), respectively. Comparison of the data indicated that the nuclear areas in DSN cells in females (XX) appear to be significantly higher than males (XY) (Figure 10H), while in male (testis) and female (ovary) phenotypes the nuclear areas appeared to be identical (Figure 10G). In PSN cells, the nuclear areas in control male (XY) and female (XX) genotypes are 8.41 ± 0.26 μm^2 ($n = 84$) and 10.67μm^2 ($n = 58$), while in male (testis) and female

(ovary) phenotypes, the area are 8.75 ± 0.25 μm^2 (n = 102) and 11.12 ± 0.64 μm^2 (n = 41), respectively. Comparisons of the data indicated that, in controls, both genotypic (XX) and phenotypic (ovary) females have significantly higher nuclear areas than the corresponding genotypic (XY) and phenotypic (testis) males (Figure 10I,J).

Exposure of the larvae to different concentrations of GO (2.5–20 mg/L) indicated that the nuclear areas (μm^2) of DSN cells in male genotypes (XY), compared to controls, were found to be significantly higher in larvae exposed to 10.0 and 20.0 mg/L GO (Figure 10G). Comparison within the larvae exposed to different concentrations of GO (2.5–20 mg) showed that, compared to 2.5 and 5.0 mg/L GO, the nuclear area of DSN cells were significantly increased (hypertrophy) in larvae exposed to both 10.0 and 20.0 mg/L GO (Figure 10G). In females (XX), compared to control larvae, significant decrease (hypotrophy) was observed in the nuclear area of DSN cells exposed to 2.5–20.0 mg/L GO (Figure 10G). Intergroup comparisons of the larvae (XX) exposed to different concentrations of GO indicated further reduction in DSN cell nuclear area in 5.0 and 20.0 mg/GO groups when compared with 2.5 mg/L GO. Further comparisons between male (XY) and female (XX) genotypes exposed to identical concentrations of GO (2.5–20 mg/L) indicated that the female genotypes (XX) exposed to 20.0 mg/L GO have significantly reduced DSN cell nuclear area than the males (XY) maintained in 20.0 mg/L GO. In phenotypes, our data indicated that the nuclear area in DSN cells of males (testis) exposed to different concentrations of GO remained at the same level as in controls, however, compared to the larvae exposed to 5.0 mg/L, significant enhancement (hypertrophy) was observed in males (testis) exposed to 10.0 or 20 mg/L GO (Figure 10H). In females (ovary), compared to controls, a significant reduction (hypotrophy) in the nuclear area of DSN cells was observed in larvae exposed to 2.5, 5.0, and 10.0 mg/L GO (Figure 10G). Further comparison of the data within the different GO-exposed groups (2.5–20 mg/L) indicated that compared to 2.5 mg/L group, the nuclear area in DSN cells were found to be significantly reduced in larvae exposed to 5.0 mg/L and enhanced in 20.0 mg/L while in 10 mg/L group the nuclear area in DSN cells appear to be significantly reduced when compared with the larvae exposed to 20 mg/L GO (Figure 10H). Further comparisons between males (testis) and females (ovary) exposed to identical concentrations of GO (2.5–20 mg/L) indicated that the phenotypic females exposed to 10.0 mg/L GO have significantly reduced DSN cell nuclear area than the males (testis) maintained in 10.0 mg/L GO. However, in contrast to 10.0 mg/L, the females (ovary) exposed to 20.0 mg/L GO have significantly higher nuclear areas than the male phenotypes exposed to identical GO concentrations (20 mg/L) (Figure 10G).

The nuclear area of the PSN cells in male genotypes (XY) exposed to 5.0, 10, and 20 mg/L GO have hypertrophic PSN cell nucleus than the larvae (XY) maintained as controls (Figure 10I). Consequently, comparisons of the data (nuclear area of PSN cells) in the larvae (XY) exposed to 2.5 mg/L GO with the larvae exposed to higher concentrations of GO (5.0–20 mg/L) indicated significant hypertrophy. While in females (XX), compared to controls, significant hypotrophy was observed in larvae exposed to 5.0 and 10.0 mg/L while remained at the same level in the larvae (XX) exposed to 2.5 and 20.0 mg/L GO (Figure 10I). Further comparisons of the data within the larvae (XX) exposed to different concentrations of GO (2.5–20 mg/L), indicated significant nuclear hypotrophy in the larvae (XX) exposed to 5.0 and 10.0 mg/L GO than the larvae (XX) in 2.5 and 20.0 mg/L GO. Moreover, to find a sex-specific differences between males (XY) and females (XX), further comparison in PSN cell nuclear area was made in the larvae exposed to equal concentrations (2.5–20 mg/L) of GO. Our data indicated that female genotypes exposed to 2.5 mg/L showed hypertrophy while in 5.0, and 10.0 mg/L showed hypotrophy in the nuclear area of PSN cells when compared with male genotypes (XY) maintained in identical GO concentrations (Figure 10I). In phenotypes, the nuclear area of PSN cells in males (testis), compared to controls, were found to be significantly increased (hypertrophy) in larvae exposed to 10.0 and 20.0 mg/L GO (Figure 10J). Further comparison within the larvae (testis) exposed to different concentrations of GO (2.5–20 mg/L), indicated significant hypertrophy in the area of PSN cells in larvae exposed to 10 and 20 mg/L GO than the larvae exposed to 2.5 and 5.0 mg/L GO (Figure 10J). In females (ovary), compared to controls, significant reductions (hypotrophy) in the nuclear area of PSN cells were observed in 2.5–10.0 mg/L GO, while in 20.0 mg/L, the nuclear area appears to be identical with the control females (ovary) (Figure 10J). Consequently, comparisons between different concentrations of GO, indicated significant decrease in larvae exposed to 10.0 mg/L and increased in larvae exposed to 20 mg/L when compared with the larvae (ovary) exposed to 2.5 and 5.0 mg/L (Figure 10J). Moreover, to indicate sex-specific effects on the nuclear area of PSN cells, further comparison was made between the male (testis) and female (ovary) phenotypes exposed to identical concentrations of GO (2.5–20 mg/L). Our data indicated that compared to male phenotypes (testis), significant hypertrophy in nuclear area of PSN cells were observed in females (ovary) exposed to 20 mg/L GO and hypotrophy in 5.0 mg/L (Figure 10J). In other GO concentrations (2.5 and 10.0 mg/L), the females (ovary), maintained the identical nuclear area (not significantly different) with male phenotypes (Figure 10J).

4 | DISCUSSION

Fish are the main vertebrate species for aquatic toxicity testing, and small fish (zebrafish, Japanese medaka, fathead minnow, and stickleback) are the main test guideline (TG) species used for testing and screening EDCs with estrogen, androgen, and steroidogenic (EAS) modalities.[2]Adrenal cortex, a steroidogenic endocrine gland, has been suggested as a toxicological target for chemicals and drugs. Depending on the dose, duration, and chemical potency of exposure, several EDCs are known to disrupt adrenocortical function and pathways.[29] The GO, an oxidized derivative of graphene, has numerous hydroxyl, carbonyl, carboxyl, and epoxy functional groups giving unique physicochemical properties and therefore the nanocarbon is widely used in different biomedical and environmental applications.[12,30] However, despite its multiple uses, several reports indicate that GO is

toxic,[17,31,32] while the potential human and ecological health risks are yet to be confirmed. Therefore, our continued studies on the evaluation of GO as an EDC utilizing the adrenal gland of Japanese medaka might be necessary.

Histologically, the adrenal gland consists of two endocrine compartments, a steroidogenic tissue originated from mesodermal mesenchyme during embryogenesis and a chromaffin tissue derived from embryonic neural crest cells.[33–35] In mammals, the adrenal gland has a peripheral cortex and an inner medulla. The cortex composed of steroidogenic tissue and produces mineralocorticoid, glucocorticoid and sex steroids under the control of HPA axis. The medulla is made up of chromaffin tissue producing mainly catecholamines under the control of sympatho-adreno-medullary system.[36,37] Although the structural anatomy of the adrenal gland in nonmammalian vertebrates is widely variable, ranging from a diffuse intermingling to a complete separation of the steroidogenic and chromaffin tissues, the biochemical characteristics and the hormones produced by the gland are mostly identical with mammals.[35]

In teleost fish, the adrenal gland is interrenal, not discrete, and the two cell types (steroidogenic interrenal cells and neuroendocrine chromaffin cells) can be mixed, adjacent or completely separated and lined on the endothelium of the posterior cardinal vein and/or its branches within the kidney.[27,38–40] Moreover, IRG is highly sensitive to toxic chemicals while there is a lack of predictability about the nature of adrenal toxicants disposed into the environment.[29,40,41] Several reports indicated that the structure and functions of the HPA-axis are disrupted in animals (fish and amphibians) living in contaminated aquatic sites.[42] Although human adrenal cell line H295R is utilized in EDC screening tests (Harvey 2016) in vitro, several chemicals including heavy metals like cadmium,[43,44] and chromium,[45] organochlorines like carbon tetrachloride,[46] and hexachlorobenzene,[47] aromatic hydrocarbons like ketoconazole[48] and etomidate[49]are the potential adrenal toxicants evaluated in different model organisms.[40,50]

To verify our hypothesis, we have used both adults and larvae of Japanese medaka fish exposed to GO either by IMR (adults and larvae) or IP (adults) and histopathological evaluations were made by following histological (HE staining), histochemical (PAS staining) and immunohistochemical (TH enzymes) methods (Figures 1–5 and 7–9; S1–S7). Moreover, for quantitative evaluation, we have counted IRG cells captured as digital images in HE stained sections and expressed the results as number of cells/mm^2 of IRG (Figures 6 and 10). In teleost, the adrenal homolog (IR axis) consists of at least two types of cells having endocrine functions (steroidogenic cells and chromaffin cells). Previously, these cells were identified by cellular morphology[27,39] or immunostaining with cell-specific enzymes such as 3β-hydroxysteroid dehydrogenase (3β-HSD) for steroidogenic cells[51] and TH for chromaffin cells.[28] In this study, we have attempted to identify the adrenal medullary cells (chromaffin cells) which express TH enzyme, the rate-limiting enzyme of catecoholamine biosynthesis.[26] However, to make it straightforward, we have divided IRG cells as DSN, having deep stained basophilic nuclei, and PSN having comparatively less basophilic nuclei than DSN (Figures S1a,b). Moreover, we have measured the nuclear area of both DSN and PSN cells and used as an indicator of cellular activity (hypo-or hypertrophy) at the IRG of medaka (Figures 6 and 10). Although our technique is not specific for steroidogenic cells, based on our hypothesis, we have reason to predict that due to high adsorbing property, GO might be nonspecifically agglomerated on the different regions of the IRG of medaka, and the sharp edge of the nanoparticle can induce cell death through necrosis/lysis that affect the structure of the organ and the hormonal status of the animal. Our studies showed that the IRG of medaka is located and lined mostly around the posterior cardinal vein or its branches within the kidney (Figures 2–5 and 7–9; S1–S7). Both DSN and PSN cells are intermingling along the IRG either in a single layer or forming clumps or cords containing 2–3 cells thick which is similar to the distribution pattern of steroidogenic (IR cells) and chromaffin cells in medaka[27] as well as in other teleost species.[39,40,52,53] Considering the age of the experimental fish, we have used reproductively active adult male and female fish for standardization of the technique based on exposure route and sex of the animal (Figures 2–6); while the larvae, depending on the genotypic and phenotypic sex, were evaluated for a concentration-dependent EDC effect of GO on IRG (Figures 7–10).

Both male and female fish as a breeding pair, exposed to GO or no GO (either by IMR or IP) in the laboratory (16 L: 8 D light cycle; 25 ± 1°C), were able to breed successfully, produced viable eggs and no death occurred in IMR fish (Figure 1). However, in IP control (vehicle-injected) fish, out of 30 breeding pairs, 6 males (20%) and 1 female (3.33%) died within 21 days post-injection period.[18,19] In addition, in IP-treated fish with 100 μg/g GO, out of 8 breeding pairs, one breeding pair (both male and female) died (12.5% male and 12.5% female) while other pairs survived and breed successfully during post-injection period. The breeding activity for males was assessed by the number of fertilized eggs produced by the breeding pair, and for females by the number of total eggs (both fertilized and unfertilized eggs) laid by the female partner.[18,19] The data indicated that a steady-state egg production was continued in both control and GO-exposed IMR fish as observed during preexposure period, however, in IP fish the controls reached a steady-state after 1 day while in GO-injected fish (100 μg/g) after one or more week days of postinjection.[18,19] We therefore predict that IP-treated fish, especially the males, were under more stressful conditions than IMR fish, which might be reflected in the basic histology of the IRG.[54]

Our histological observations in adult fish indicated that the impairments of IRG in the experimental male and female fish are dependent on the route of exposure of the nanomaterial. Compared to fish maintained as IMR, the effects are more pronounced in IP-treated fish and GO aggravated the process (Figures 2,3). In both males and females, the arrangement of IRG cells, especially as a cord, appears to be distorted in IP fish (Figures 3A–D). Moreover, when exposed to GO, compared to IMR (Figure 3E–H), a severe distortion was noticed intermittently in IRG of both male and female IP fish (Figures 3E–F and S2a,b). The sinusoidal space became increased and the cords appear to become hypertrophied and dumbbell-shaped in appearance in several regions of IRG (Figure S2a,b). Although to our knowledge, the evaluation of GO as an EDC targeting IRG of fish has not been done yet, our histological data are more or less similar with

the observations made in *Channa punctatus*, where the arrangement pattern of IRG in cords was distorted and the spaces (lacunae) between the cords of IR axis cells were decreased due to cellular hypertrophy and degranulation after chromium (20–40 mg/L, 96 h) exposure.[45] Our histochemical evaluation showed that the IRG cells in Japanese medaka are PAS negative and GO exposure (both IMR and IP) did not show any significant variation in PAS activity in these cells (Figure 4). Available reports indicated that the IRG cells of *Labeo rohita*, *Pimephales promelas*, *Anabas scandens*, and *Brycon cephalus* are found to be PAS negative,[55,56] while in reed-fish some of the IRG cells are PAS positive.[57] In *Cirrhinus mrigala* (Ham.) cortical cells exhibited weak response to PAS, while chromaffin cells in *Labeo*, *Cirrhinus*, and *Puntius sophore*, showed moderately intense PAS reaction.[58,59] In Nile tilapia, some of the interrenal cells and the noradrenaline-containing chromaffin cells are PAS positive, while adrenaline-containing chromaffin cells are not.[53] From our immunohistochemical studies, although we are unable to distinguish adrenaline or nor-adrenaline cells, we predict that the observed TH positive cells in IRG of Japanese medaka adults and larvae are chromaffin cells and their distribution adjacent to the endothelium of the cardinal veins passing through the head kidney indicated the specific location of the IRG in the head kidneys of a teleost (Figures 5 and 9). Taken together, from our histopathological studies, we simply predict that GO exerts a negligible effect on the PAS positivity and metabolic activity of IRG cells of Japanese medaka, even though structural impairments of IRG cannot be ruled out.

For quantitative evaluation of the impairments made by GO in the structure (cellular distribution) and functions (nuclear area) of IRG, we have compared cellular distribution (number of cells/mm^2) and the nuclear area (μm^2) of the IRG cells of medaka adults (both males and females) exposed with and without GO (control), adopting two routes of exposure (IMR and IP-injection) (Figure 1). Previously, we have observed that the significant number of adults Japanese medaka males were died after IP-injection of vehicle than females.[18,19] In the current experiment, we expect a gender-specific effects of GO in Japanese medaka depending on the route of exposure (IMR vs. IP), even though we expect that the amount of GO available to the IRG cells of medaka adults by these two routes (20 mg/L in IMR and 100 μg/g in IP) might be identical. Although inconsistent, our data indicate that the fish exposed to GO (either through IMR or IP), have significantly reduced IRG cells and enhanced nuclear hypertrophy in both male and female fish (Figure 6). When considered all cells (DSN + PSN), if the exposure route was immersion, GO (20 mg/L, IMR) was found to be ineffective, while in IP route, GO was able to significantly reduce the number of IRG cells in both male and female fish (Figure 6A). Considering DSN cells, gender-specific effect of GO was observed only in male fish in both exposure routes (IMR and IP) (Figure 6B), while in PSN cells, GO was able to significantly reduced only in females if the exposure route was IP (Figure 6C). Considering nuclear area, both in DSN and PSN cells, significant nuclear hypertrophy was observed in both male and female fish, if the fish immersed in GO (20 mg/L, IMR); in IP fish, hypertrophic nuclei in DSN cells were observed only in male fish, while in PSN cells, both male and female fish have hypertrophic nuclei (Figure 6D,E). Although the effects of GO is inconsistent in our experimental model, we still predict that the impairments made by GO on IRG is nonspecific and probably due to agglomeration of GO on the organ entered into the body of the fish through either of the exposure routes (IMR or IP).

Our histological and histochemical studies indicate that the structural and biochemical features of the IRG of Japanese medaka make the organ an ideal target of EDCs.[41,42] Exposures to pollutants, including pulp and paper effluents, metals, polychlorinated biphenyl (PCB) and chlordane exhibited hypertrophy and hyperplasia of the IRG cells in fish.[42,60] Moreover, other factors related to stress are also altered the cytophysiology of IRG cells. Depending on the annual reproductive cycle for maintaining a steady-state hormonal balance, the male stickleback (*Gasterosteteus aculeatus*), can periodically renew and replace mitochondria and smooth endoplasmic reticulum (SER) in the IRG cells.[61] In cichlid fish, *Cichlasoma dimerus*, the steroidogenic cells in the IRG have comparatively greater nuclear area (hypertrophy) in non-territorial males (lowest social rank) than territorial (dominant pre-spawning) males.[54] Taken together, our studies indicated that the structural impairment and the nuclear hypertrophy of the IRG induced in adult male and female medaka, exposed to GO either by IMR or IP, are probably mediated through stress-related imbalance in circulating cortisol level in fish.[42]

To evaluate the concentration-dependent effect of GO on the IRG of medaka, we have extended our studies further in medaka larvae by analyzing interrenal tissue of the same experimental fish used in our previous experiment.[20,21] The larvae were exposed to different concentrations of GO (2.5–20 mg/L), continuously for 96 h by IMR and evaluated after 6 weeks of depuration in a GO-free environment. We have also observed that GO accumulated in the gut of the larvae in a concentration-dependent manner.[20,21] For histological, histochemical, immunohistochemical, and quantitative evaluation of IRG (Figures 7–9), we followed the same strategies as we did in the adult fish (Figures 2–5). Our histological data indicate similarities in the structure and location of the IRG of larvae and adult fish and GO induced occasional impairments which are not restricted to a specific region of the IRG (Figure 7A–F). Moreover, histochemical and immunohistochemical studies indicated that the IRG cells in larvae are PAS negative (Figure 8A–F), and immunoreactive to TH enzyme (Figure 9A–F).

During quantitative analysis, despite our focus on the concentration-dependent effects of GO, we have also assessed its effect on gender specificity as male (XY) and female (XX) genotypes as well as male (testis) and female (ovary) phenotypes. As the secondary sexual features were yet to develop in the larvae on 47th dph, the sex of the larvae was determined by phenotypic (histological examination of the gonads either as testis or ovary) and genotyping (XY and XX) methods.[20–23] We have observed that ~27% male phenotypes instead of XY genotypes, were XX (8 XX larvae have testis out of 29 larvae with phenotypic testis), and we considered these larvae as sex-reversed during our previous studies on gonads[20,21] and thyroids.[22,23] In the present study, we are unable to track the IRG of all the experimental larvae. Therefore, the larvae having testis as gonad

are considered as male phenotypes (testis) and the larvae genotyped XX were considered as females, irrespective of the presence of testis or ovary.

Our data indicated that the number of IRG cells (total cells; DSN + PSN) and the nuclear area of DSN and PSN cells in the larvae of male (XY) and female (XX) genotypes (Figure 10A) or male (testis) and female phenotypes (ovary) (Figure 10B) appear to be higher than the adult males or females (Figure 6A,D,E). Although we do not know the exact reason for this age-specific difference (larvae vs. adults), we expect that the circulating cortisol level of these fish may not be identical between these two age groups (larvae and adults). In our experimental fish, we did not measure the circulating cortisol level, however, we expect that the differences in gonadal maturity in these fish (adults and larvae) might alter the hormonal status that affect the structure and functions of the IRG cells which are responsible for the maintenance of circulating cortisol level through HPA axis.[29,42] In male stickleback, the variation in the structure and functions of the IRG cells and thus the circulating cortisol level are linked to the different periods of the annual reproductive cycle.[61]

Although we used only one concentration (20 mg/L) or dose (100 μg/g) of GO in adult fish, to observe a concentration-dependent EDC response of GO, medaka larvae (1 dph) were exposed to four different concentrations of GO (2.5, 5.0, 10.0, and 20.0 mg/L) continuously for 96 h and evaluated on 47th dph after 6 weeks depuration.[20,21] However, the toxic effects we have observed on the IRG of larvae were inconsistent and very hard to evaluate GO as an AED. We believe that like adults, in larvae, GO could be non-specifically agglomerated on the IRG and infrequently lysed the cells which might be reflected on the effects of GO we observed in our current experiments.

5 | CONCLUSIONS

Overall, our experimental results on histopathology of the IRG (adrenal homolog of mammals) in Japanese medaka adults, either immersed in 20 mg/L or IP-injected with 100 μg/g GO and evaluated after 3 weeks (21 days) depuration and on larvae (1st fry stage), exposed to four different concentrations of (2.5, 5.0, 10.0, and 20.0 mg/L for 96 h), did not specifically establish GO as an AED even though the structural impairments of the organ were observed. Moreover, our studies based on histology, histochemistry and immunohistochemistry, indicated that in both adults and larvae, the IRG is located adjacent to the endothelium of the cardinal veins passing through the head kidney. Further, our data on the quantitative evaluation of the IRG cell sorting indicated that the route of exposure, age, and sex of the fish need to be critically considered during the evaluation of a chemical as an AED. Although in the present study, we did not focus of the HPA axis, we expect that structural impairments induced by GO could directly or indirectly disrupt the HPA axis which will be reflected on the circulating cortisol level of the fish.

AUTHOR CONTRIBUTIONS

Asok K. Dasmahapatra: conceptualization, formal analysis, investigations, methodology, project administration, writing-original manuscript; Paul B. Tchounwou: conceptualization, funding acquisition, project administration, resources, supervision, writing and editing manuscript.

ACKNOWLEDGMENTS

The research was supported by NIH/NIMHD grant # G12MD07581 (RCMI Center for Environmental Health), NIH/NIMHD grant #1U54MD015929 (RCMI Center for Health Disparities Research), and NSF grant #HRD 1547754 (CREST Center for Nanotoxicity Studies) at Jackson State University, Jackson, Mississippi, USA.

CONFLICT OF INTEREST

The authors declare no conflicts of interest.

ORCID

Asok K. Dasmahapatra https://orcid.org/0000-0003-4924-4762
Paul B. Tchounwou https://orcid.org/0000-0002-3407-6674

REFERENCES

1. Krimsky S. The unsteady state and inertia of chemical regulation under the US toxic substances control act. *PLoS Biol*. 2017;15:e2002404.
2. OECD. *Revised Guidance Document 150 on Standardized Test Guidelines for Evaluating Chemicals for Endocrine Disruption, OECD Series on Testing and Assessment*. OECD Publishing,. 2018; 10.1787/9789264304741-en.
3. Karthikeyan BS, Ravichandran J, Mohanraj K, Vivek-Anath RP, Samal A. A curated knowledgebase on endocrine disrupting chemicals and their biological systems-level perturbations. *Sci Total Environ*. 2019;692:281-296.
4. Dzeiwiecka M, Witas P, Karpeta-Kaczmarek J, et al. Reduced fecundity and cellular change in archeta domesticus after multigenerational exposure to graphene oxide nanoparticle in food. *Sci Total Environ*. 2018;635:947-955.
5. Zheng P, Wu N. Fluorescence and sensing applications of graphene oxide and graphene quantum dots: a review. *Chem Asia J*. 2017;12:2243-2353.
6. Benelli G. Mode of action of nanoparticles against insects. *Environ Sci Pollut Int*. 2018;25:12329-12341.
7. Dasari Shreena TP, McShan D, Dasmahapatra AK, Tchounwou PB. A review on graphene-based nanomaterials in biomedical applications and risks in environment and health. *Nano-Micro lett*. 2018;10(3):53.
8. Pena-Bahamonde J, Nguyen HN, Fanourakis SK, Rodrigues DF. Recent advances in graphene-based biosensor technology with applications in life sciences. *J Nanobiotechnology*. 2018;16:75. doi:10.1186/s12951-018-0400-z
9. Avant B, Bouchard D, Chang X, et al. Environmental fate of multi-walled carbon nanotubes and graphene oxide across different aquatic ecosystems. *NanoImpact*. 2019;13:1-12.
10. Li D, Wang T, Li Z, Xu X, Wang C, Duan Y. Application of graphene-based materials for detection on nitrate and nitrite in water-a review. *Sensors*. 2020;20:54.
11. Ren W, Cheng H-M. The global growth of graphene. *Nature Nanotech*. 2014;9:726-730.
12. Marchi LD, Pretti C, Gabriel B, Marques PAAP, Freitas R, Neto V. An overview of graphene materials: properties, applications and toxicity

on aquatic environments. *Sci Total Environ*. 2018;631–632:1440-1456.
13. Sanchez VC, Jachak A, Hurt RH, Kane AB. Biological interactions of graphene-family nanomaterials- an interdisciplinary review. *Chem Res Toxicol*. 2012;25:15-34.
14. De March L, Neto V, Pretti C, et al. Physiological and biochemical impacts of graphene oxide in polychaetes: the case of diopatra neapolitana. *Comp Biochem Physiol C Toxicol Pharmacol*. 2017;193:50-60.
15. Li M, Zhu J, Wang M, Fang H, Zhu G, Wang Q. Exposure to graphene oxide at environmental concentrations induces thyroid endocrine disruption and metabolic disturbance in *Xenopus laevis*. *Chemosphere*. 2019;236:124834.
16. Evariste L, Mottier A, Pinelli E, Flahaut E, Gauthier L, Mouchet F. Graphene oxide and reduced graphene oxide promote the effects of exogenous T3 thyroid hormone in amphibian *Xenopus laevis*. *Chemosphere*. 2021;281:130901.
17. Dasmahapatra AK, Dasari TPS, Tchounwou PB. Graphene-based nanomaterial toxicity in fish. *Rev Environ Int*. 2019;130:104928.
18. Dasmahapatra AK, Powe DK, Dasari TPS, Tchounwou PB. Assessment of reproductive and developmental effects of graphene oxide on Japanese medaka (*Oryzias latipes*). *Chemosphere*. 2020;259:127221. 10.1016/chemosphee.2020.127221
19. Dasmahapatra AK, Powe DK, Dasari TPS, Tchounwou PB. Experimental data sets on the characterization of graphene oxide and its reproductive and developmental effects on Japanese medaka (*Oryzias latipes*) fish. *Data Brief*. 2020;32:106218. doi:10.1016/j.dib.2020.10628
20. Myla A, Dasmahapatra AK, Tchounwou PB. Sex-reversal and histopathological assessment of potential endocrine disrupting effects of graphene oxide on Japanese medaka (*Oryzias latipes*) larvae. *Chemosphere*. 2021;279:130768. doi:10.1016/j.chemosphere.2021.130768
21. Myla A, Dasmahapatra AKTPB. Experimental data sets on sex-reversal and histopathological assessment of potential endocrine disrupting effects of graphene oxide on Japanese medaka (*Oryzias latipes*) larvae at the onset of maturity. *Data Brief*. 2021;38:107330. doi:10.1016/j.dib.2021.107330
22. Asala TE, Dasmahapatra AK, Myla A, Tchounwou PB. Experimental data sets on the evaluation of graphene oxide as a thyroid endocrine disruptor and a modulator of gas gland cells in Japanese medaka (*Oryzias latipes*) larvae at the onset of maturity. *Data Brief*. 2021;39:107625.
23. Asala TE, Dasmahapatra AK, Myla A, Tchounwou PB. Histological and histochemical evaluation of graphene oxide on thyroid follicles and gas gland of Japanese medaka larvae (*Oryzias latipes*). *Chemosphere*. 2022;286:131719.
24. Iwamatsu T. Stages of normal development in the medaka *Oryzias latipes*. *Mech Dev*. 2004;121:605-618.
25. Mullick Chowdhury S, Dasgupta S, McElroy AE, Sitharaman B. Structural disruption increases toxicity of graphene nanoribbons. *J Appl Toxicol*. 2014;34:1235-1246.
26. Daubner SC, Le T, Wang S. Tyrosine hydroxylase and regulation of dopamine synthesis. *Arch Biochem Biophys*. 2011;508:1-12.
27. Oguri M. Histo-morphology of the kidney and adrenal gland of medaka, *Oryzias latipes* (T.ET S.). *Bull Jap Soc. Sci Fish*. 1961;17:1058-1062.
28. Shin S-W, Chung N-I, Kim J-S, et al. Effect of diazinon on behavior of Japanee medaka (*Oryzias latipes*) and gene expression of tyrosine hydroxylase as a biomarker. *J Environ Sci Health*. 2001;B36:783-795.
29. Harvey PW. Adrenocortical endocrine disruption. *J Sterois Biochem Mol Biol*. 2016;155:199-206.
30. Zhang T, Tremblay P-L. Graphene: an antibacterial agent or a promoter of bacterial proliferation ? *iSci*. 2020;23:101787. 10.1016/j.sci.2020.101787
31. Ema M, Hougaard KS, Kishimoto A, Honda K. Reproductive and developmental toxicity of carbon-based nanomaterials: a literature review. *Nanotoxicology*. 2016;10:391-412.
32. Malhotra N, Villaflores OB, Audira G, et al. Toxicity studies on graphene-based nanomaterials in aquatic organisms: current understanding. *Molecules*. 2020;25:3618.
33. Carballeira A, Fishman LM. The adrenal functional unit: a hypothesis. *Perspect Biol Med*. 1980;23:573-597. 10.1353/pbm.1980.0064
34. De Falco M, Laforgia V, Valiante S, Virgilio F, Varano L, De Luca A. Different patterns of expression of five neuropeptides in the adrenal gland and kidney of two species of frog. *Histochem J*. 2002;34:21-26. 10.1023/A:1021387623735
35. Di Lorenzo M, Barra T, Rosati L, et al. Adrenal gland response to endocrine disrupting chemicals in fishes, amphibians and reptiles: a comparative overview. *Gen Comp Endocrinol*. 2020;297:113550.
36. Nicolaides NC, Kyratzi E, Lamprokostopoulou A, Chrousos GP, Chrmandari E. Stress, the stress system and the role of glucocorticoids. *Neuroimmunomodulation*. 2015;22:6-19. 10.1159/000362736
37. Berger I, Werdermann M, Bornstein SR, Steenblock C. The adrenal gland in stress adaptation on a cellular level. *J. Steroid Biochem Mol. Biol*. 2019;190:198-206.
38. Butler DG. Structure and function of the adrenal gland of fishes. *Amer Zool*. 1973;13:839-879.
39. Gallo VP, Civinini A. Survey of the adrenal homolog in teleosts. *Int Rev Cytol*. 2003;230:89-187.
40. Hontela A, Vijayan MM. Adrenocortical toxicology in fishes. In: P.W. Harvey, D.J. Everett, C.J. Springall (Eds.) *Adrenal Toxicology*, Informa HealthcareClick here to enter text., 2009, pp.233–256.
41. Lauretta R, Sansone A, Sansone M, Romanelli F, Appetecchia M. Endocrine disrupting chemicals: effects of endocrine glands. *Front Endocrinol*. 2019;10:178. doi:10.3389/fendo.2019.00178
42. Lorenzo MD, Barra T, Rosati L, et al. Adrenal gland response to endocrine disrupting chemicals in fishes, amphibians and reptiles: a comparative overview. *Gen Comp Endocrinol*. 2020;297:113550.
43. Mgbonyebi OP, Smothers CT, Mrotek JJ. Modulation of adrenal cell functions by cadmium salts, 5. Cadmium acetate and sulphate effects on basal and ACTH-stimulated steroidogenesis. *Cell Boil Toxicol*. 1998;14:301-311.
44. Lacroix A, Hontella AA. A comparative assessment of the adrenotoxic effects of cadmium in two teleost species, rainbow trout, onconrhynchus mykiss and yellow perch, Peca flavescens. *Aqua Toxicol*. 2004;67:13-21.
45. Mishra AK, Mohanty B. Effect of hexavalent chromium exposure on the pituitary-interrenal axis of a teleost, *Channa punctatus* (Bloch). *Chemosphere*. 2009;76:982-988.
46. Borgan WC, Eacho PI, Hinton DE, Colby HD. Effects of carbon tetrachloride on adrenocortical structure and function in Guinea pigs. *Toxicol Appl Pharmacol*. 1984;75:118-127.
47. De Coster S, van Larebeke N. Endocrine-disrupting chemicals: associated disorders and mechanisms of action. *J Environ Public Health*. 2012;2012:713696. doi:10.1155/2012/713696
48. Engelhardt D, Weber MM, Miksch T, Abedinpour F, Jaspers C. The influence of ketoconazole on human adrenal steroidogenesis: incubation studies with tissue slices. *Clinc Endocrinol*. 1991;35:163-168.
49. Wagner RL, White PF, Kan PB, Rosenthal MH, Feldman D. Inhibition of adrenal steroidogenesis by the anaesthetic etomidate. *New Eng J Med*. 1984;310:1415-1421.
50. Hinson JP, Raven PW. Effects of endocrine-disrupting chemicals on adrenal function. *Best Pract Res Clic Endocrinol Metabol*. 2006;20:111-120.
51. Chou C-W, Lin J, Hou H-Y, Liu Y-W. Visualizing the interrenal steroidogenic tissue and its vascular microenverionment in zebrafish. *J Vis Exp*. 2016;118:e54820. doi:10.3791/54820
52. Civinini A, Gallo VP. Degeneration and possible renewal processes related to the interrenal cells in the head kidney of the stickleback Gasterosteus aculeatus. *Tissue Cell*. 2007;39:109-122.

53. Gaber W, Abdel-maksoud FM. Interrenal tissue, chromaffin cells and corpuscles of Stannius of Nile tilapia (*Oreochromis niloticus*). *Microscopy*. 2019;68:195-206.
54. Morandini L, Honji RM, Ramallo MR, Moreira RG, Pandolfi M. The interrenal gland in males of the cichlid fish *Cichlasoma dimerus*: relationship with stress and the establishment of social hierarchies. *Gen Comp Endocrinol*. 2014;195:88-98.
55. Kulkarni RS, Sathyanesan AG. Adrenal histochemistry of the freshwater teleost *Labeo rohita* (ham.). *Aral Anat E Embriol*. 1979;84:171-181.
56. Rocha RM, Leme-Dos Santos HS, Vicentini CA, Da Cruz C. Structural and ultrastructural characteristics of interrenal gland and chromaffin cells of matrinxa, *Brycon cephalus* Gunther 1869 (Teleostei-Characidae). *Anat Histol Embryol*. 2001;30:351-355.
57. Yosun JH, Butler OG, Bawks BA. Distribution and structure of the adrenocortical homolog in the reed-fish (*Calarnoichthys calabaricus* smith). *Acta Zool (Stockh)*. 1988;69:77-86.
58. Kulkarni RS, Sathyanesan AG. Cytochemical and histoenzymological studies on the adrenal of the teleost, *Puntius sophore* (ham.). *Z Mikrosk Anat Forsch*. 1978;92:529-540.
59. Joshi BN, Sathyanesan AG. A histochemical study on the adrenal components of the teleost *Cirrhinus mrigala* (ham.). *Z Mikrosk Anat Forsch*. 1980;94:327-336.
60. Norris DO, Felt SB, Woodling JD, Dores RM. Immunocytochemical and histological differences in the interrenal axis of feral brown trout, Salmo trutta, in metal-contaminated waters. *Gen Comp Endocrinol*. 1997;108:343-351.
61. Civinini A, Padula D, Gallo VP. Ultrastructural and histochemical study on the interrenal axis cells of the male stickleback (Gasterosteus aculeatus, teleostea), in relation to the reproductive annual cycle. *J Anat*. 2001;199:303-316.

SUPPORTING INFORMATION

Additional supporting information can be found online in the Supporting Information section at the end of this article.

How to cite this article: Dasmahapatra AK, Tchounwou PB. Histopathological evaluation of the interrenal gland (adrenal homolog) of Japanese medaka (*Oryzias latipes*) exposed to graphene oxide. *Environmental Toxicology*. 2022;37(10):2460-2482. doi:10.1002/tox.23610